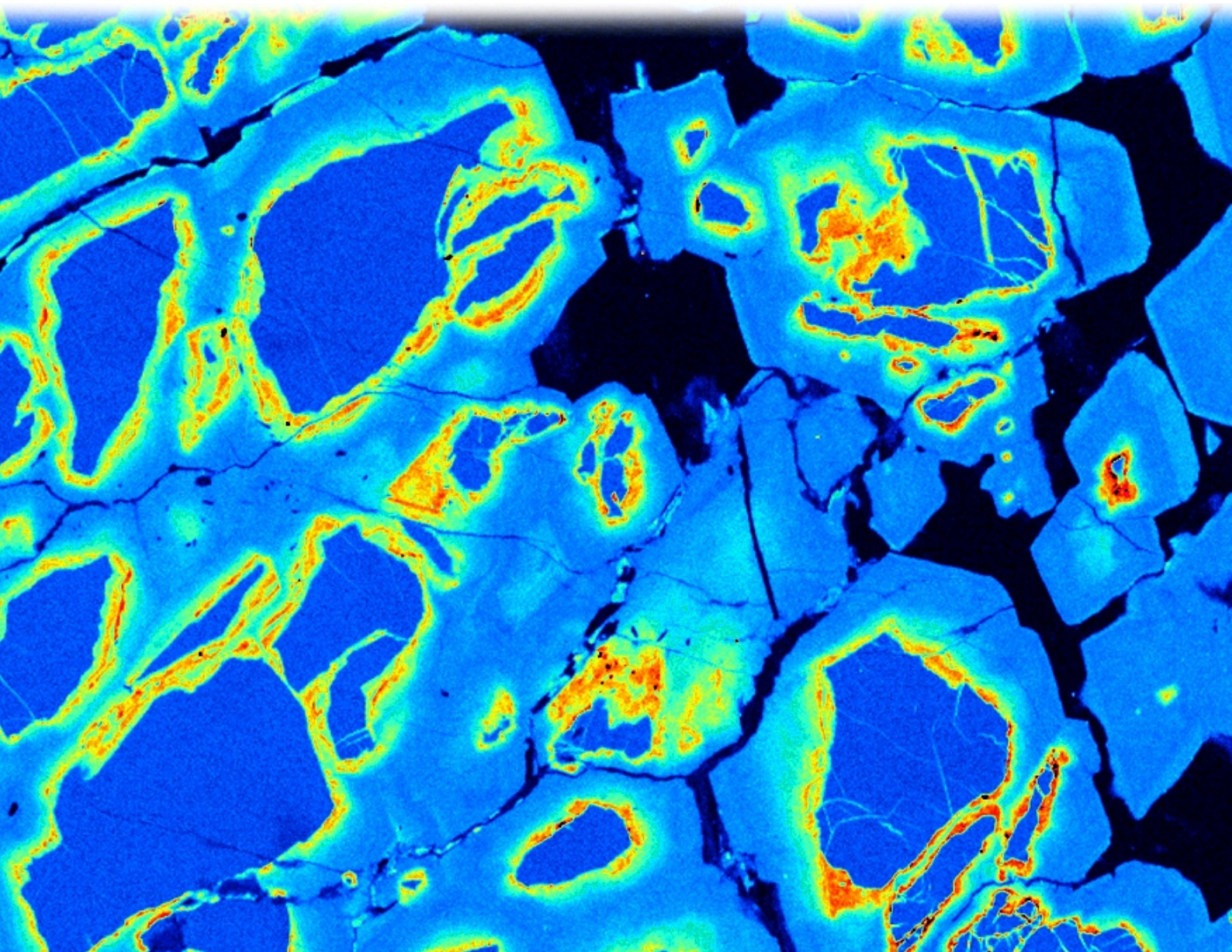


Chemical and isotopic records of polycyclic histories in a subducted continental crust (Dora-Maira Massif, Western Alps)

Francesco Nosenzo



Chemical and isotopic records of polycyclic histories in a subducted continental crust (Dora-Maira Massif, Western Alps)

Francesco Nosenzo

Academic dissertation for the Degree of Doctor of Philosophy in Geology at Stockholm University to be publicly defended on Friday 21 April 2023 at 10.00 in William-Olssonsalen, Geovetenskapens hus, Svante Arrhenius väg 8.

Abstract

At convergent plate margin, part of the continental crust can be subducted and exhumed. During continental subduction a pre-existing crust is reworked. Remnants of an older orogen are recycled and subjected to (ultra)-high-pressure metamorphism. During subduction, polycyclic rocks undertake a second metamorphic cycle, whereas monocyclic rocks are metamorphosed for the first time. In reworked rocks the pre-subduction record is overprinted and partially or completely lost. Despite this difficulty, reconstructing the pre-subduction history of the recycled crust is crucial, because pre-subduction characters (such as H₂O content) can strongly influence how rocks respond to reworking during subduction.

The Dora-Maira Massif is worldwide renowned as a (ultra)-high-pressure continental terrane. However, its northern part remained essentially unexplored in recent times. In this thesis work the northern Dora-Maira Massif is used as a case study to investigate recycling of continental crust. The aim is to constrain what type of crust is subducted and exhumed and to unravel the role of fluids during subduction of polycyclic material. Field work, petrology, thermodynamic modelling and geochronology are integrated.

New field and geochronological evidence indicate that the northern Dora-Maira Massif displays an internal architecture more complex than what previously thought. It is subdivided in several tectonic units likewise the southern Dora-Maira Massif. Chemical and isotopic records of the reworked rocks reveal a pre-Alpine history spanning from the Lower Palaeozoic to the Mesozoic. A polycyclic basement preserves relicts of a pre-Alpine Barrovian metamorphism connected with the Variscan orogenesis. The absence of granulite-facies partially molten pre-Alpine rocks indicates that only the upper crust was reworked in the Dora-Maira Massif.

Thermodynamic modelling indicates that polycyclic micaschists were rehydrated between the Variscan and the Alpine peak metamorphism. Polycyclic garnet texture and chemistry and metamorphic zircon record a main episode of fluid infiltration at the end of the Variscan cycle and not during the Alpine cycle. Pre-Alpine re-hydration of the upper crust allowed high-pressure re-equilibration during subduction.

Keywords: *Subduction, continental crust, polycyclic, garnet, metamorphic petrology.*

Stockholm 2023

<http://urn.kb.se/resolve?urn=urn:nbn:se:su:diva-215338>

ISBN 978-91-8014-226-7
ISBN 978-91-8014-227-4

Department of Geological Sciences

Stockholm University, 106 91 Stockholm



CHEMICAL AND ISOTOPIC RECORDS OF POLYCYCLIC HISTORIES IN A
SUBDUCTED CONTINENTAL CRUST (DORA-MAIRA MASSIF, WESTERN ALPS)

Francesco Nosenzo

Chemical and isotopic records of polycyclic histories in a subducted continental crust (Dora-Maira Massif, Western Alps)

Francesco Nosenzo

©Francesco Nosenzo, Stockholm University 2023

ISBN print 978-91-8014-226-7

ISBN PDF 978-91-8014-227-4

Printed in Sweden by Universitetservice US-AB, Stockholm 2023

Cover picture: X-ray map of Ca showing polycyclic garnet textures (field of view 0.6 x 0.5 mm); image processing by Marin Robyr

When I was a kid, one of my friends once said: "I heard that **minerals grow**; did you know?". One other kid jumped into the conversation and said: "that's utter nonsense!".

The claim certainly sounded weird to me, but my friend seemed sure about it. I was curious and I wanted to find out the truth. So, skeptical but fascinated by the idea, I went on to perform my first geoscientific inquiry. I had a quartz crystal at home. I stared at it for weeks and months, checking if it would grow in size over time. I even came back to the crystal a few years later, only to find out that it had always remained the same... It even looked smaller than before; perhaps I had grown up in the meantime.

Now I know that my friend spoke the truth, despite my experiment seemed to tell otherwise. Minerals can grow, but only under very special conditions.

Abstract

At convergent plate margin, part of the continental crust can be subducted and exhumed. During continental subduction a pre-existing crust is reworked. Remnants of an older orogen are recycled and subjected to (ultra)-high-pressure metamorphism. During subduction, polycyclic rocks undertake a second metamorphic cycle, whereas monocyclic rocks are metamorphosed for the first time. In reworked rocks the pre-subduction record is overprinted and partially or completely lost. Despite this difficulty, reconstructing the pre-subduction history of the recycled crust is crucial, because pre-subduction characters (such as H₂O content) can strongly influence how rocks respond to reworking during subduction.

The Dora-Maira Massif is worldwide renowned as a (ultra)-high-pressure continental terrane. However, its northern part remained essentially unexplored in recent times. In this thesis work the northern Dora-Maira Massif is used as a case study to investigate recycling of continental crust. The aim is to constrain what type of crust is subducted and exhumed and to unravel the role of fluids during subduction of polycyclic material. Field work, petrology, thermodynamic modelling and geochronology are integrated.

New field and geochronological evidence indicate that the northern Dora-Maira Massif displays an internal architecture more complex than what previously thought. It is subdivided in several tectonic units likewise the southern Dora-Maira Massif. Chemical and isotopic records of the reworked rocks reveal a pre-Alpine history spanning from the Lower Palaeozoic to the Mesozoic. A polycyclic basement preserves relicts of a pre-Alpine Barrovian metamorphism connected with the Variscan orogenesis. The absence of granulite-facies partially molten pre-Alpine rocks indicates that only the upper crust was reworked in the Dora-Maira Massif.

Thermodynamic modelling indicates that polycyclic micaschists were rehydrated between the Variscan and the Alpine peak metamorphism. Polycyclic garnet texture and chemistry and metamorphic zircon record a main episode of fluid infiltration at the end of the Variscan cycle and not during the Alpine cycle. Pre-Alpine re-hydration of the upper crust allowed high-pressure re-equilibration during subduction.

Sammanfattning

Vid en konvergerande plattgräns kan delar av jordskorpan bli subducerad eller exhumerad. Vid kontinental subduktion sker en omvandling av jordskorpan där relikter från tidigare orogener blir återcirkulerade och genomgår (ultra)-högtrycksmetamorfos. Vid denna process genomgår polycykliska bergarter en andra cykel av metamorfos medan monocykliska bergarter blir metamorfoserade för första gången. Då bergarter omvandlas blir spår av tidigare metamorfa cykler överpräglade vilket medför svårigheter för rekonstruering. Det är dock viktigt att undersöka den geologiska bakgrunden före subduktionen, eftersom egenskaper ärvda från tidigare cykler (till exempel andelen H_2O) har en stor betydelse på hur bergarter blir omvandlade under subduktion.

Dora-Maira Massivet är världskänt för dess (ultra)-högtryckskaraktär, men trots detta är den norra delen av massivet till stor del utforskat. I denna studie undersöktes den norra delen av Dora-Maira Massivet för att studera omarbetning av kontinentalskorpan under subduktion. Syftet är att ta reda på vilken typ av jordskorpa som blir subducerad och exhumerad samt att granska betydelsen av fluider vid subduktion av polycykliska bergarter. Den nu presenterade studien omfattar fältarbete, petrologi, termodynamisk modellering och geokronologi.

Norra Dora-Maira Massivet visade sig ha en mer komplex uppbyggnad än man tidigare trott. I likhet med den välstuderade södra delen av massivet kan det delas in i ett flertal tektoniska enheter. Kemiska analyser och isotopanalyser indikerar att de omvandlade bergarterna har en pre-Alpisk historia som sträcker sig från äldre Paleozoikum till Mesozoikum. Den polycykliska berggrunden bevarar relikta mineral som indikerar pre-Alpisk metamorfos av Barrovian-typ under den Variskiska orogensen. Avsaknaden av partiellt uppsmälta pre-Alpiska höggradigt metamorfoserade bergarter tyder på att endast den övre delen av jordskorpan blev omvandlad i Dora-Maira Massivet.

Termodynamisk modellering indikerar att de polycykliska skifferbergarterna rehydrerades i perioden mellan den Variskiska och den Alpiska metamorfosen. Textur och kemi bevarad i polycykliska granater, och metamorfa zirkoner indikerar att fluidinfiltration skedde vid slutet av den Variskiska, och inte under den Alpiska cykeln. Detta ledde till att den övre delen av jordskorpan nådde en ny jämvikt under högt tryck under subduktionen.

Preface

The present doctoral thesis is a compilation of three scientific papers. The first part of the thesis is the *kappa*, which provides an overlook on the conducted research project. The *kappa* is intended for the non-specialist reader, although it goes in some depth into the subject matter. The second part comprises the three attached papers, referred to as Paper I, II and III.

The *kappa* is structured in the following manner. In the introduction, the reader is given the background knowledge of what is known about the subject matter and what remains unsolved. Then, the reader is introduced to the regional geology of the studied area. The scientific questions and the specific research objectives are then highlighted. Subsequently, the theoretical framework of the methods used and the logic behind their application to the research aims is laid out. Details on the methodology, such as laboratory working conditions, can be found in the attached papers. The main results of the thesis are presented in a logic succession, not necessarily following the order of the three papers. Finally, the key conclusions and their implications are discussed.

Included papers

Paper I:

Nosenzo, F., Manzotti, P., Pujol, M., Ballèvre, M., & Langlade, J. (2022). A window into an older orogenic cycle: *P–T* conditions and timing of the pre-Alpine history of the Dora-Maira Massif (Western Alps). *Journal of Metamorphic Geology*, 40(4), 789–821.
<https://doi.org/10.1111/jmg.12646>.

Paper II:

Nosenzo, F., Manzotti, P., & Robyr, M. (under review). H₂O budget and metamorphic re-equilibration in polycyclic rocks as recorded by garnet textures and chemistry. *Lithos*.

Paper III:

Nosenzo, F., Manzotti, P., Ballèvre, M & Pujol, M. (manuscript). Tectonic architecture of the northern Dora-Maira Massif (Western Alps, Italy): field and geochronological evidence. To be submitted to *Swiss Journal of Geosciences*.

Author's contribution

Paper I: FN, PM and MB took part in the field work. FN prepared the microprobe analyses by selecting the sites of measurement on minerals of interest at the scanning electron microscope (SEM). Microprobe analyses were performed in different laboratories by FN, PM and JL, using the documentation prepared by FN. MB performed local chemical analyses at the SEM following documentation prepared by FN. FN conducted sample preparation for X-ray fluorescence (XRF) analyses. Victoria Pease (PetroTectonic analytical facility, Stockholm University) performed XRF analyses. FN conducted thermodynamic modelling. FN separated zircons from the selected samples and prepared the mount for laser-ablation ion-coupled-plasma mass-spectrometry (LA-ICP-MS). FN and PM identified monazite at the scanning electron microscope (SEM) and mapped its location in the thin sections, in preparation for LA-ICP-MS. The Covid pandemic impeded FN to conduct LA-ICP-MS analyses himself; therefore, MP and MB performed the analyses using the documentation prepared by FN. FN and MP conducted isotopic data processing. FN wrote the manuscript with step-wise review by PM and MB and final review by the other co-authors.

Paper II: Further study was carried out on samples partly investigated in paper I and on a new sample collected during previous field work. FN prepared the SEM documentation for microprobe and MR performed the analyses. FN performed measurements of local chemical composition at the SEM. FN conducted sample preparation for XRF and Victoria Pease performed the analyses. FN conducted loss on ignition (LOI) sample preparation and measurements. FN carried out thermodynamic modelling. FN wrote the manuscript with step-wise review by PM and final review by MR.

Paper III: FN, PM and MB conducted extensive field work as a team. FN separated zircons from the selected samples and prepared the mount for LA-ICP-MS. FN and MP performed the analyses and data processing. FN wrote the manuscript with step-wise review by PM and MB and final review by MP.

FN: Francesco Nosenzo; PM: Paola Manzotti; MP, Marc Poujol; MB: Michel Ballèvre; JL: Jessica Langlade; MR: Martin Robyr.

Contributions not included in this thesis

Manzotti, P., Schiavi, F., **Nosenzo, F.**, Pitra, P., & Ballèvre, M. (2022). A journey towards the forbidden zone: a new, cold, UHP unit in the Dora-Maira Massif (Western Alps). *Contributions to Mineralogy and Petrology*, 177, 59.

Table of contents

1. Introduction	1
1.1 Tectonic evolution of convergent plate margins	1
1.2 Metamorphism as a record of subduction, exhumation and collision	2
1.3 Continental subduction	3
1.4 Mechanisms and drivers of continental subduction and exhumation	4
1.5 Reworking of pre-existing continental crust	5
1.6 The role of fluids during metamorphism	5
1.7 H ₂ O budget of subducted polycyclic crust	7
1.8 Garnet as a record of metamorphic evolution and polycyclic histories	8
2. Geological settings	9
2.1 The Alpine Belt	9
2.2 The Dora-Maira Massif	9
3. Scientific questions	11
4. Methodology	12
4.1 Field work	12
4.2 Petrography and mineral chemistry	12
4.3 Bulk-rock geochemistry	13
4.4 Thermodynamic modelling	14
4.4.1 Isochemical phase diagrams	15
4.4.2 H ₂ O conditions and T - $M(H_2O)$ diagrams	17
4.4.3 Limitations and corrections	17
4.5 Geochronology and trace element geochemistry	18
4.5.1 U-(Th)-Pb dating	19
4.5.2 Protolith age of meta-sediments: detrital zircon	20
4.5.3 Interpreting metamorphic ages: petrochronology	21
4.5.4 Laser-ablation ion-coupled-plasma mass-spectrometry (LA-ICP-MS)	22
5. Results and interpretation	23
5.1 Geology of the northern Dora-Maira Massif: lithologies, age of the protoliths and tectonic architecture (paper I and III)	23
5.1.1 Pinerolo Unit	23
5.1.2 Chasteiran Unit	24
5.1.3 Muret unit	24
5.1.4 Serre Unit	25
5.2 Petrology of weakly and strongly reworked polycyclic rocks (paper I and II)	25
5.3 Polycyclic garnet textures (paper I and II)	27
5.4 P - T conditions and timing of the pre-Alpine cycle (paper I)	29
5.5 P - T conditions of the Alpine cycle (paper II)	31
5.6 H ₂ O budget and rehydration of polycyclic micaschists (paper II)	33
6. Conclusions and implications for continental subduction	35
6.1 Reworking of pre-existing continental crust during subduction	35
6.1.1 Subduction of crustal fragments	35
6.1.2 Reworking of upper crust	36
6.2 The role of H ₂ O during subduction of polycyclic crust	36
References	38
Acknowledgements	49

1. Introduction

1.1 Tectonic evolution of convergent plate margins

Plate tectonics, theorized by Wegener (1912) as “continental drift” and broadly accepted after oceanic spreading was demonstrated (Vine & Matthews, 1963), is responsible for shaping the external portion of our rocky planet. For example, mountain belts (or orogens), one of the most prominent features on Earth’s surface, represent the final product of convergent tectonics. The tectonic evolution of convergent plate margins is summarized below (e.g. Kearey et al., 2009; Frisch et al., 2011).

Before convergence, oceanic crust is generated at the mid-oceanic ridge and separates two continental plates with their respective passive margins (Fig. 1). As convergence commences, the denser oceanic crust and the attached lithospheric mantle starts to subduct either below another segment of oceanic crust or below one of the two continental plates. Geophysical evidence allows direct observation of ongoing oceanic subduction. For example, seismicity is recorded along the subduction plane, even at great depth (up to ~ 600 km; Green et al., 1994). The oceanic crust mostly sinks into the mantle and is lost at depth. However, a few slices may detach from the downgoing slab and be brought back towards the surface in a process called exhumation. Hereafter the term “subduction” (both oceanic and continental) is used to indicate burial of rocks to great depth (typically mantle depths), regardless if they are then lost into the mantle or exhumed. The oceanic crust initially contains abundant H₂O, due to interaction with seawater along the mid-oceanic ridge. During subduction, the oceanic crust progressively dehydrates and releases H₂O. H₂O percolates in the mantle wedge above the subduction zone where it triggers partial melting (e.g. Schmidt & Poli, 1998). As a result, the upper plate is affected by abundant magmatism, with the development of an island arc in the case of an ocean-ocean collision or of an active continental margin in the case of an ocean-continent collision (Fig. 1).

If convergence continues, the entire oceanic crust is subducted and the two continents collide. According to most tectonic models, subduction ceases at this stage although it is now broadly accepted that the continental crust can be subducted as well (see section 1.3; Fig. 1). Continent-continent collision implies pervasive deformation of the continental crust, with thrusting and stacking of several distinct crustal volumes, or nappes, derived from both of the upper and the lower plates. As a result, the continental crust thickens, leading to isostatic uplift and formation of a mountain belt. The late stage of continental collision is often associated with widespread magmatism.

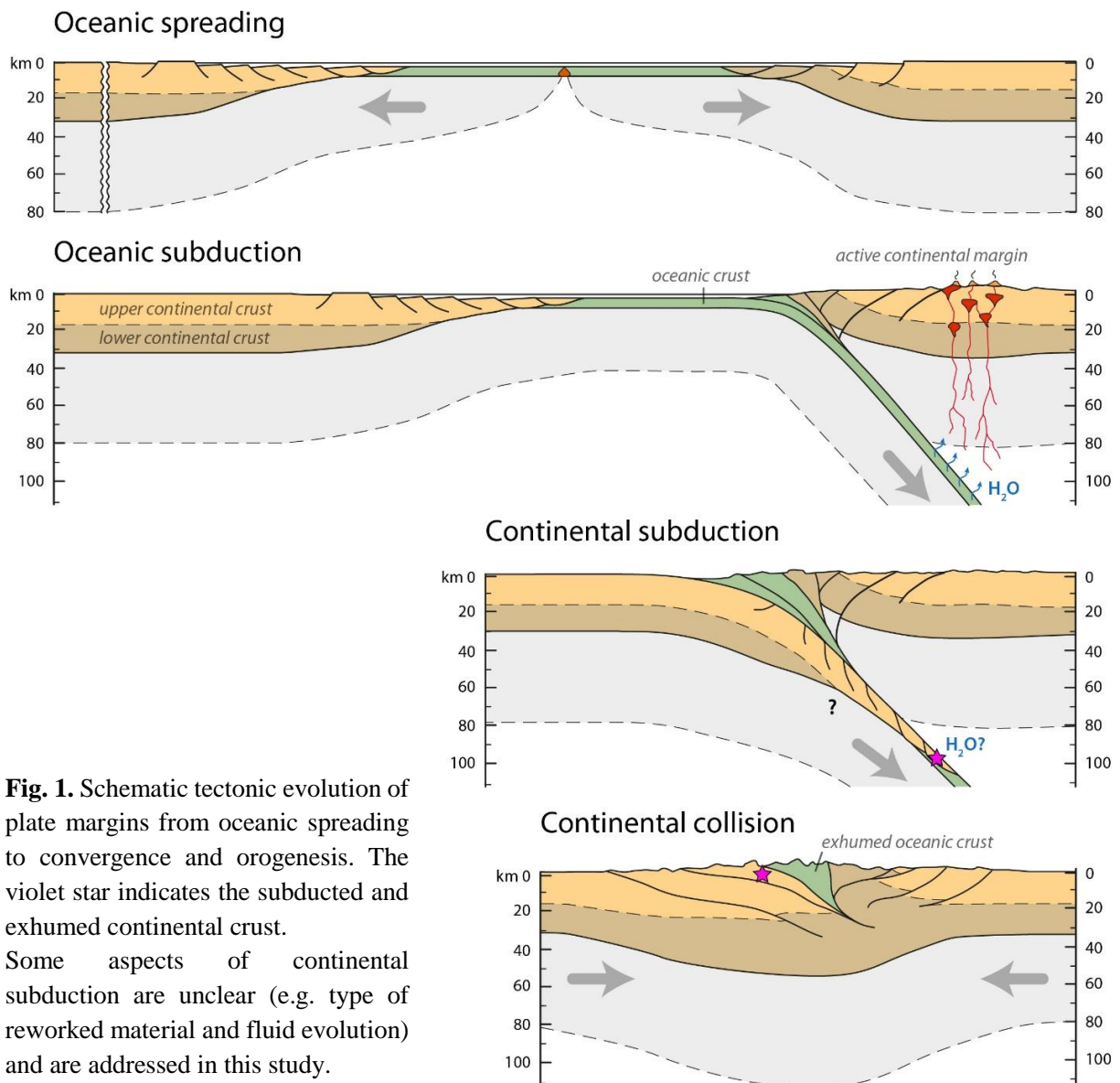


Fig. 1. Schematic tectonic evolution of plate margins from oceanic spreading to convergence and orogenesis. The violet star indicates the subducted and exhumed continental crust. Some aspects of continental subduction are unclear (e.g. type of reworked material and fluid evolution) and are addressed in this study.

1.2 Metamorphism as a record of subduction, exhumation and collision

Reworking of the oceanic and continental crust during convergence is accompanied by metamorphic transformations in response to changes in pressure and temperature ($P-T$). Therefore, the $P-T$ history of the rocks record the unique fingerprint of their tectonic evolution.

P and T increase with depth. In fact, lithostatic P is a function of the weight of the overlying rock column (i.e. the overburden) and T follows the geothermal gradient. During subduction, cold crustal material (both oceanic and continental) is brought at great depth, where the surrounding

rocks are much hotter. However, heating of the subducting crust is delayed due to the poor thermal conductivity of rocks, especially if subduction is fast. As a result, during subduction, burial follows a “cold” geotherm ($\leq 10^\circ\text{C}/\text{km}$) and rocks are metamorphosed at high-pressure (*HP*) but generally low-temperature (*HT*) conditions. If the *P* conditions exceed the coesite stability field (> 27 kbar; equivalent to more than ~ 85 km depth) they are considered ultra-high (*UHP*). At the maximum depth, rocks reach peak *P* conditions. Subsequently, during exhumation, rocks undergo decompression and their *HP* mineralogy can be overprinted by a low-pressure (*LP*) one. The first stages of decompression are often isothermal but can also be accompanied by a *T* decrease or increase. The tectonic and metamorphic evolution described above is referred to as the subduction-exhumation cycle.

During continental collision a “hotter” geotherm ($\sim 30^\circ\text{C}/\text{km}$) is generally established. As such, in some orogens (e.g. in the Himalaya and the Caledonides; Liou et al., 2004; Lang & Gilotti, 2015) exhumation of subducted crust may be accompanied by overprinting of the (U)*HP* mineralogy by a *LP–HT* one. During continental collision, other slices of continental crust that were not subducted can be underthrust and buried within the thickened crust. As a result, rocks undergo the classic Barrovian metamorphic sequence (Barrow, 1893) and can reach high-temperature (*HT*) but generally low-pressure conditions (*LP*). Partial melting and magmatism in the lower crust is common during continental collision. After this *LP–HT* event the crust can be exhumed and cooled down, with overprinting of the *HT* mineralogy by a low-temperature (*LT*) one. Metamorphism in response to heating (occurring during subduction and burial) is referred to as prograde, whereas re-equilibration in response to cooling is referred to as retrograde.

1.3 Continental subduction

In most textbooks (e.g. Kearey et al., 2009; Frisch et al., 2011), tectonic models of convergent plate margins depict subduction exclusively for the oceanic crust. By contrast, the continental crust has been traditionally considered too light to subduct (McKenzie, 1969). However, the occurrence of *HP–UHP* continental terranes in many orogens worldwide testifies that the continental crust can also be subducted and exhumed. It was in the Alps that continental subduction was first postulated in the 1950s (Amstutz, 1951), although the tectonic nappe architecture had been recognized as early as the 1910s (Ampferer, 1906; Argand, 1916). The discovery of coesite in some continental units of the Alps (in the Dora-Maira Massif; Chopin, 1984) and the Caledonides (Smith, 1984) proved for the first time that the continental crust could reach great depth (> 100 km). Today, seismic imaging has detected subducted continental slabs beneath the Pamir (Schneider et al., 2013) and the Alps (Zhao et al., 2015).

Given its low density, it is generally thought that the subducted continental crust cannot be lost into the mantle; instead, it must be completely exhumed and accreted to the orogenic wedge. In other words, it is usually assumed that mass balance is maintained before and after continental

subduction (and collision). However, Ingalls et al. (2016) suggested that in the Himalayan Belt up to 50% of the pre-collisional continental crust may have been subducted and lost into the mantle.

1.4 Mechanisms and drivers of continental subduction and exhumation

The mechanisms and drivers of continental subduction and exhumation are still controversial. The presented thesis work does not aim to address such issues directly, but represents a contribution towards a comprehensive understanding of continental subduction.

How can the low-density continental crust ($\sim 2.8 \text{ g/cm}^3$) be buried into the high-density mantle ($\sim 3.3 \text{ g/cm}^3$)? In fact, even after *HP-UHP* metamorphism the continental crust remains mostly lighter than the mantle ($3.0\text{--}3.2 \text{ g/cm}^3$; own estimates calculated with Theriak-Domino and results from Engi et al., 2018). It is generally thought that the continental crust is pulled (or dragged) at depth by the subducting oceanic slab (e.g. Burov et al., 2012). Exhumation requires detachment from the downgoing slab. Given the low density of the continental crust, buoyancy is considered the main driver of exhumation, whereas erosion plays a minor role (Yamato et al., 2008; Guillot et al., 2009; Burov et al., 2012; Butler et al., 2014; Schmalholz & Schenker, 2016). However, the tectonic mechanism that allows continental material to be exhumed by buoyancy forces is yet to be clarified.

Numerical simulations (or models) can be used to unravel the behaviour and tectono-metamorphic history of the continental crust during subduction and exhumation. However, current numerical models face severe challenges in trying to reproduce the conditions observed in *HP-UHP* continental terranes found in nature. For example, *UHP* units are generally smaller in volume and were exhumed faster than what the models predict (Schenker et al., 2015; Engi et al., 2017). In an attempt to reconcile natural observations with numerical models, some authors have recently proposed an alternative interpretation for the genesis of *UHP* continental terranes. They suggest that the continental crust can never be subducted to great depth; instead it undergoes *UHP* metamorphism at shallower depth, under the effect of tectonic overpressure (e.g. Li et al., 2010; Schmalholz & Podladchikov, 2014; Gerya, 2015). In other words, metamorphic *P* recorded in rocks is not purely lithostatic, but is also affected by tectonic (differential) stresses. Many arguments in favour of tectonic overpressure are based on the detection of *P* differences in adjacent rock volumes not only at the scale of the orogen, but also at the outcrop scale (e.g. Luisier et al., 2019; Putnis et al., 2021). However, (apparent) variations in *P* estimates in different lithologies and domains may also be the result of differential development and preservation of the peak mineralogy. Therefore, understanding the conditions which regulate metamorphic re-equilibration and recording of the *P–T* evolution (such as fluid conditions; see section 1.6) has important tectonic implications.

1.5 Reworking of pre-existing continental crust

Orogenic events occur cyclically throughout Earth's history. The Wilson cycle starts with rifting of the continental crust and ends with collision of the two continental margins. At the end of the cycle, the continental crust mainly consists of a metamorphosed basement intruded by magmatic bodies. The continental crust can be divided into an upper portion, comprising low-grade or non-metamorphosed rocks of generally felsic composition, and a lower portion comprising high grade and partially molten rocks of generally more intermediate and mafic composition (Fig. 1). A new Wilson cycle begins with rifting of the sutured continent and subsequent opening of a new ocean. During rifting the continental crust is extended and a passive margin develops. Sedimentary covers, recording crustal thinning and subsidence, are deposited on top of the basement. After a period of oceanic spreading, the tectonic regime is inverted and convergence commences. During the ensuing continental subduction, this heterogeneous pre-existing crust is reworked. A reworked metamorphic basement is referred to as polycyclic because it experienced more than one orogenic and metamorphic cycle, whereas reworked magmatic rocks and sedimentary covers are referred to as monocyclic.

What part of the pre-existing continental crust is subducted and exhumed remains unclear. One hypothesis is that only the thinned distal margin may be subducted. By contrast, the proximal part of the margin may be too thick and too buoyant and, thus, it may block the subduction zone. However, geophysical observations below the Pamir indicate the occurrence of a thick continuous slab of subducted continental crust (Schneider et al., 2013). Such observations combined with other tectonic models (Doin & Henry, 2001; Ingalls et al., 2016) suggest that only the lower crust is subducted, whereas the upper crust is decoupled from the lower crust at shallow depth and accreted to the orogenic wedge. Other models (Jolivet et al., 2005; Guillot et al., 2009) suggest that both the upper and lower crust are subducted, but only the former is exhumed. *HP-UHP* terranes found in nature contain both reworked upper crustal material (e.g. Liou et al., 2004; Rolfo et al., 2004; Liu et al., 2009) and lower crustal material (Austrheim, 1987; Engi et al., 2018)

In summary, investigating what type of continental material was subducted and exhumed may have key implications for understanding the tectonic mechanisms at play. To understand this, the pre-subduction history of *HP-UHP* terranes should be reconstructed. This can be challenging, as subducted and exhumed rocks underwent pervasive deformation and metamorphism, with overprinting of the pre-subduction record.

1.6 The role of fluids during metamorphism

Rocks are an aggregate of solids phases (i.e. minerals), but they can also contain fluids within the pore space between crystals and in fractures. Porosity values, expressed as voids per unit volume, are in the range 0.5–2.0 vol% for igneous and metamorphic rocks, when not pervasively fractured (e.g. Thompson & Connolly, 1990; Tullborg & Larson, 2006; Rao et al., 2022). The fluid phase

can consist of different chemical components and it can contain (and transport) dissolved elements. H₂O is the most common fluid component but also CO₂ can be locally abundant (e.g. during metamorphism of carbonates). Hereafter we consider aqueous fluids only (i.e. consisting solely of H₂O).

Consider a thermodynamic system consisting of a rock volume undergoing metamorphism. Fluids are free to flow in and out of the system and their availability strongly controls metamorphic re-equilibration. During metamorphism fluids interact with the rest of the rock in two different ways:

(i) They accelerate reaction rates by lowering the activation energy (kinetic role of H₂O; Pattison et al., 2011). Fluids act as a reaction catalyst, mediating mineral dissolution and precipitation, and facilitating intergranular transport of dissolved chemical components (e.g. Rubie, 1986; Milke et al., 2013). Ion diffusivities are several orders of magnitude higher in presence of fluids (Carlson, 2010; Gardés et al, 2012), especially when the pores are interconnected and completely fluid-filled (a condition referred to as fluid-saturation). By contrast, in the absence of fluids, rocks may remain unreactive (metastable) and escape metamorphic re-equilibration (e.g. Austrheim, 1987; Wain et al., 2001).

(ii) H₂O in the fluid phase acts as a chemical component of the system (thermodynamic role of H₂O; Pattison et al., 2011). H₂O can be incorporated into the crystal lattice of hydrous minerals and as such it takes part in metamorphic reactions as a product or reactant. This is exemplified by the following dehydration reaction (e.g. Inui & Toriumi, 2004):



During this reaction the hydrous mineral chlorite is consumed to form garnet and the H₂O chemically bounded in chlorite is liberated to form a free fluid phase. Because the rock lost a fraction of H₂O originally bounded to the solid phases, we can say that the rock dehydrated. In pelites, dehydration reactions typically occur during subduction and prograde metamorphism. Anhydrous minerals are thermodynamically favoured over hydrous minerals at higher *T*. Fluids released during the prograde metamorphism of pelites enhance reaction kinetics and self-sustain metamorphic re-equilibration. The fluids in excess tend to escape the system and migrate upward towards the surface or laterally, following anisotropies and preferential fluid pathways such as fractures (e.g. Walther & Oreville, 1982; Ferry & Gerdes, 1998; Connolly, 2010). Conversely, during retrograde metamorphism and exhumation, H₂O must be added to the system from an external source in order to re-transform garnet into chlorite. As a general rule, meta-pelites develop and preserve their peak mineral assemblage, provided that they do not interact with externally-derived fluids during exhumation and cooling (Guiraud et al., 2001; Proyer, 2003). Other lithologies, such as meta-granites, may exhibit an opposite behaviour, dehydrating during decompression and cooling. As a result, the peak *HP* assemblage may not be preserved or even recorded in meta-granites (Proyer, 2003; Young & Kylander-Clark, 2015; Schorn, 2022).

In summary, the P – T record of a rock may be incomplete due to the presence or absence of fluids at certain stages of the subduction-exhumation cycle. Fluids regulate the development and preservation of the peak HP mineral assemblage. Therefore, estimation of the peak P – T conditions and, in turn, of the maximum burial depth (assuming lithostatic P) should consider the fluid evolution and its effect on metamorphic re-equilibration.

1.7 H₂O budget of subducted polycyclic crust

As mentioned in section 1.1, it is well-known that oceanic subduction is accompanied by a release of large quantities of H₂O from the subducting slab (Fig. 1). By contrast, fluid circulation at continental subduction zones has been poorly investigated to date. Consider a polycyclic continental crust metamorphosed during a first orogenic cycle and subsequently subducted during a second orogenic cycle. Two end-member models of fluid-rock interactions during subduction have been proposed.

(i) According to one model, the subducting crust remains a closed system with respect to external fluid infiltration (Tenczer et al., 2006; Schorn, 2018). The H₂O that can be used to promote metamorphic re-equilibration during subduction is constrained to the amount that can be extracted from the hydrated minerals contained in the rocks. This internally-derived H₂O content, hereafter referred to as H₂O budget, is inherited from the pre-subduction history (i.e. the first orogenic cycle). Depending on the H₂O budget, the subducting crust may show different behaviours. If the H₂O budget is low (e.g. due to dehydration as a result of the first cycle), the crust may remain dry during subduction, hindering the development of the HP mineral assemblage. If the H₂O budget is high enough (e.g. due to rehydration at the end of the first cycle), the mineral-bound H₂O may be released enhancing re-equilibration at HP conditions. In this latter case the polycyclic crust may act as a fluid source during subduction.

(ii) The second model suggests that externally-derived fluids interact with the crust at depth, during subduction (Angiboust et al., 2017; Bhowany et al., 2018; Engi et al., 2018; Vho et al., 2020). Serpentinites (Vho et al., 2020) and meta-sediments (Mattey et al., 1994) undergoing dehydration at greater depth have been proposed as possible sources of such fluids. Fluid infiltration may be localized along fractures and shear zones (Austrheim, 1987; Zertani et al., 2019) and may be linked to seismicity along the subduction plane (Lund & Austrheim, 2003; Austrheim, 2013). Externally-derived fluids allow re-equilibration at HP conditions, whereas internally-derived fluids (those extracted from the H₂O budget) play a minor role. According to this model a dry polycyclic crust is rehydrated during subduction, acting as a fluid sink.

Discerning which of the two models better describes the fluid evolution at continental subduction zones has important implications for recording of the P – T evolution (and thus of the burial depth and gradients), seismicity, rheology (e.g. Austrheim et al., 1997; Bjørnerud et al., 2002; Malvoisin et al., 2020) and ore formation (e.g. talc and gold; Sandrone et al., 1987; Pettke et al., 2000).

1.8 Garnet as a record of metamorphic evolution and polycyclic histories

Garnet is a key mineral for metamorphic petrologists. It commonly occurs across a wide range of protolith compositions and P – T conditions. It generally forms porphyroblasts and during its growth it can include a large number of other crystals. The study of inclusions allows us to infer the coexistence of garnet with other minerals. Garnet can also include accessory minerals that can be used for geochronology (such as monazite; see section 4.5.3). Garnet microstructures in a foliated rock (such as porphyroblasts wrapped by the foliation) are excellent indicators of the relative timing of deformation (e.g. Passchier & Trouw, 2005).

Garnet displays a wide range of chemical compositions, being a solid solution of four main end-members. Its composition varies in function of the P – T conditions of equilibration, as garnet exchanges cations with other minerals. For example, garnet and biotite exchange Fe^{2+} and Mg^{2+} , with the former mineral becoming increasingly richer in Mg towards higher T and vice versa. Therefore, it is possible to constrain the T of equilibration of the garnet-biotite pair knowing their composition, using a calibrated geothermometer (Ferry & Spear, 1978). However, in most cases, garnet growth is not instantaneous, but occurs continuously along a segment of the P – T path. As a result, garnet will develop compositional zoning from core to rim. This makes garnet an exceptional chemical record of the P – T evolution. Garnet can record more than one orogenic cycle, with the development and preservation of multiple generations (polycyclic garnet; e.g. Gaidies et al., 2006; Cutts et al., 2010). Detrital garnets, overgrown by a second garnet generation have also been described (Manzotti & Ballèvre, 2013).

In most cases, garnet grows during the prograde evolution and is consumed during the retrograde evolution, according to (e.g.) reaction (1) (section 1.6). During retrogression, fluid infiltration promotes garnet replacement by chlorite. Therefore, garnet textures can be used as a proxy for fluid-rock interactions, providing insights into the history of hydration and dehydration of the rock (e.g. Baxter & Caddick, 2013).

In summary, these characteristics make garnet the perfect tool to unfold the polycyclic history of the rock, including episodes of fluid-rock interactions.

2. Geological setting

2.1 The Alpine Belt

In the aftermath of Mesozoic rifting of Pangea and oceanic spreading, the Piemonte-Liguria Ocean divided the European passive margin to the west from the Adriatic one to the east. The Alpine orogeny is the result of subduction of the Piemonte-Liguria Ocean below the Adriatic plate and subsequent collision with the European plate, occurring throughout the Upper Carboniferous and the Cenozoic (e.g. Schmid et al., 2004; Handy et al., 2010; Handy et al., 2021). Slices of oceanic material were exhumed after reaching great depth (up to ~ 100 km, as recorded e.g. by the *UHP* Lago di Cignana Unit; Groppo et al., 2009). The oceanic units are now sandwiched between the Adria-derived units above and the Europe-derived ones below (Fig. 2). Also part of the European distal margin, referred to as Briançonnais Domain or micro-continent, was subducted and exhumed. Subduction of Briançonnais continental crust is recorded in the *HP* to *UHP* Internal Crystalline Massifs (ICM), now exposed as tectonic windows below the oceanic units, in the more internal part of the Western Alpine Belt. From north to south, the ICM are the Monte Rosa, the Gran Paradiso and the Dora-Maira (Fig. 2). To the difference of other *HP-UHP* terranes in other orogenic belts (e.g. the Caledonides and the Himalaya), the ICM were not affected by the late Barrovian *HT* overprint and, thus, represent an ideal case study to investigate the subduction history.

2.2 The Dora-Maira Massif

The Dora-Maira Massif in the South-Western Alps (Italy) extends for ~ 75 km from north to south and for ~ 30 km from west to east (Fig. 2). Among the three ICM, the Dora-Maira Massif is the only one known to contain *UHP* rocks. Coesite-bearing rocks were discovered in the southern sector of the massif by Chopin (1984). Since then, the southern Dora-Maira Massif has been object of studies, mostly focused on *P-T* conditions and timing of the Alpine metamorphism. The internal architecture of the southern Dora-Maira Massif consists of a stack of several tectonic units which differ for Alpine peak *P-T* conditions, ranging from garnet-blueschist-facies to coesite-eclogite-facies, and in part for lithology (Chopin et al., 1991; Compagnoni et al., 2012; Groppo et al., 2019). The age of the Alpine peak metamorphism is comprised between 40 and 33 Ma (Rubatto & Hermann, 2001; Bonnet et al., 2022).

Until recently, the northern Dora-Maira Massif remained essentially unexplored. Available tectonic maps are mostly based on early large-scale studies (scale 1:100000, Mattiolo et al., 1913, 1951; Vialon, 1966). Although these old maps generally provide a reliable indication on the geographical distribution of the main lithologies, they were made at a time when the theory of plate tectonics and thermobarometry were still in their infancy and thus were interpreted solely on

a lithostratigraphic basis. Two tectonic units are traditionally recognized in the northern Dora-Maira Massif: a lower unit (the Pinerolo Unit), characterized by monocyclic meta-sediments (Manzotti et al., 2016) and meta-intrusives (Bussy & Cadoppi, 1996), and an upper unit, mainly comprising a polycyclic basement and minor monocyclic covers (Sandrone et al., 1993; Gasco et al., 2011). Alpine peak P - T conditions are considered to have reached garnet-blueschist-facies in the lower unit and quartz eclogite-facies in the upper unit (Borghi et al., 1985; Gasco et al., 2011), although modern dedicated studies are lacking.

In the polycyclic units of the northern and southern Dora-Maira Massif, pre-Alpine metamorphism is documented by numerous pre-Alpine relicts (e.g. Chopin et al., 1991; Compagnoni & Rolfo, 2003), but has never been characterized for P - T evolution and age. In the Punta Muret area (northern sector), contrasting studies advocate for different pre-Alpine conditions: Cadoppi (1990) described amphibolite-facies relicts, such as pseudomorphs after staurolite, whereas Bouffette et al. (1993) mentioned potential granulite-facies relicts, such as pseudomorphs after sillimanite.

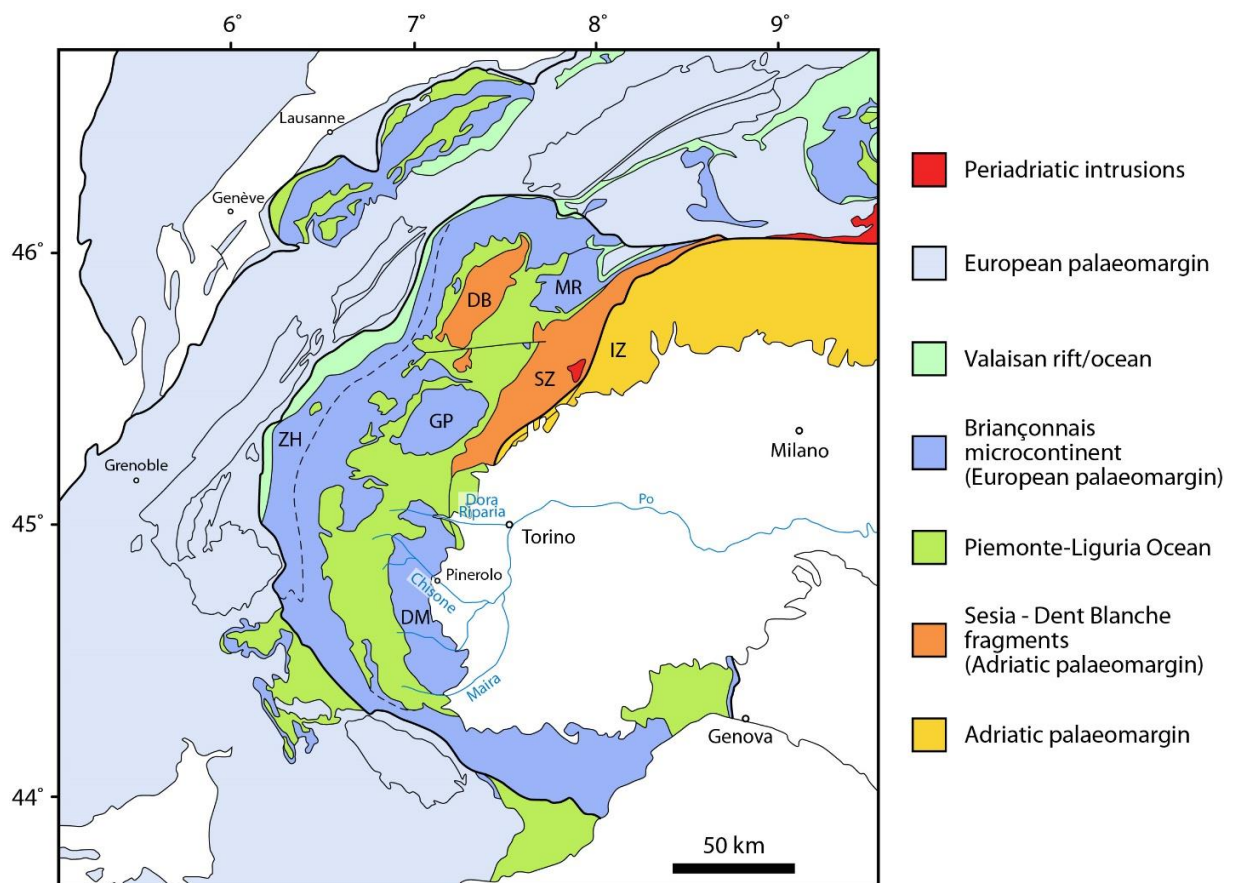


Fig. 2. Tectonic and palaeogeographic map of the Western and Central Alps (modified from Schmid et al., 2004; Ballèvre et al., 2018). MR = Monte Rosa, GP = Gran Paradiso, DM = Dora-Maira, IZ = Ivrea Zone, SZ = Sesia Zone, DB = Dent Blanche, ZH = Zone Houlliere.

3. Scientific questions

1. The pre-subduction history of reworked continental crust (papers I and III):

What type of continental material is subducted and exhumed?

An older basement or younger sedimentary covers?

Monocyclic or polycyclic material?

The upper crust or the lower crust?

To tackle these questions, the following specific research aims were considered:

- Establishing the tectonic architecture of the northern Dora-Maira Massif and comparing it to the southern sector.
- Characterizing type and age of the protoliths.
- Determining P - T evolution and age of the pre-Alpine metamorphic cycle in polycyclic rocks.

2. The role of fluids during subduction of polycyclic material (paper II):

Is the H_2O content inherited from the former orogenic cycle (i.e. the H_2O budget) enough to allow recording of the HP overprint during the second cycle?

Is the polycyclic crust dehydrated (fluid source) or hydrated (fluid sink) during subduction?

To tackle these questions, the following specific research aims were addressed:

- Determining the P - T -fluid conditions of the Alpine overprint in polycyclic meta-pelites.
- Retracing the H_2O budget evolution throughout the pre-Alpine and Alpine cycles in polycyclic meta-pelites.
- Using polycyclic garnet textures and geochronology to assess the conditions and timing of fluid-rock interactions.

4. Methodology

4.1 Field work

Because updated geologic maps of the northern Dora-Maira Massif were lacking, initial field work aimed at establishing the lithostratigraphic and tectonic architecture of the northern Dora-Maira Massif. Particular attention was dedicated to deformation and the occurrence in the field of key metamorphic minerals, such as garnet (one or two generations) and pseudomorphed staurolite. New tectonic units were discovered and characterized mainly on the basis of the identification of tectonic boundaries and on lithostratigraphy. New tectonic units were given the name of the type locality where the characteristic features can be observed.

The studied area (~ 55 km²), located in the South-Western Alps (Italy), mainly comprises the northern slope of the Germanasca valley and the Burcet Valley (two tributary valleys of the Chisone Valley). Geological mapping was conducted on topographic base maps at the 1:10000 scale (*Carta Tecnica Regionale*, CTR). Field data were digitalized and used to generate a geologic map. More than 250 samples were collected systematically within the area.

4.2 Petrography and mineral chemistry

From the collected samples, several petrographic thin sections were made. A few samples, exhibiting a polycyclic evolution, were selected for in-depth petrologic investigation (papers I and II; Table 1). Meta-pelites (i.e. micaschists) were preferred, as they tend to develop key metamorphic minerals (e.g. garnet, staurolite, chloritoid) and microstructures. In addition, micaschists are the predominant lithology in the polycyclic units, allowing extrapolation of the result from the micro- and meso-scale to the macro-scale.

The petrographic study focused on establishing the sequence of mineral growth in relation with deformation in polycyclic samples. Detail study of the microtextures was conducted with the scanning electron microscope (SEM) at the Swedish Museum of Natural History (NRM, Stockholm). Quantitative measurement of the mineral composition was carried out by electron microprobe (EMP) at the University of Oslo, at the University of Lausanne and at the Microsonde Ouest (Brest). In order to decode the complex internal zoning of garnet, compositional profiles and element maps were generated.

SEM and EMP analyses are based on the same physical principles; however, the latter is more precise, accurate and has generally higher elemental resolution (e.g. Reed, 2005). Both instruments bombard the sample (e.g. a thin section) with a high-energy electron beam, generated from a central column (Fig. 3a). The ionizing beam scatters the electrons in the inner orbitals of the atoms constituting the sample, leaving a vacancy. The vacancy is immediately filled by electrons in more external orbitals or by free (unbound) electrons. In this process, a photon, in the X-ray range, is

emitted. The wavelength of the photon is a function of the energy difference between orbitals, which, in turn, depends on the structure of the emitting atom. The measurement (e.g. with a wavelength-dispersive detector) of the wavelength of the emitted photon allows identification of the elements present in the analysed material (e.g. a mineral). Quantification of the elemental proportions is done by calibration against one or more standard materials of known composition.

	Lithology	Sampling domain	Mineral chemistry	Pre-Alpine $P-T$ conditions	Alpine $P-T-H_2O$ conditions	Age and chem. of the protolith	Age of pre-Alpine metamorphism
OG9	Clapier orthogneiss	High-strain domain				X	
OG34	Granero orthogneiss	High-strain domain				X	
OG36	Granero orthogneiss	High-strain domain				X	
OG27	Muret orthogneiss	Low-strain domain	X			X	
GM1	Garnet-staurolite micaschist	Low-strain domain (far from fractures)	X	X	X	X	X
GM2	Garnet-staurolite micaschist	Low-strain domain (close to fractures)	X		X		
GM13	Garnet micaschist	High-strain domain	X	X	X	X	

Table 1. Summary of samples studied in depth. The investigated samples were collected in the Muret Unit, except sample OG9 (Serre Unit).

4.3 Bulk-rock geochemistry

The bulk-rock composition of selected samples was measured with different scopes. Orthogneiss samples were analysed in order to determine the major element geochemistry of their magmatic protolith (papers I and III). These results are considered qualitative, because major elements may have been remobilized during metamorphism. The major element composition of micaschist samples was used for isochemical phase diagram calculation (papers I and II).

The composition of a large rock volume (referred to as whole rock composition) was obtained by X-ray fluorescence (XRF). XRF analysis is based on the same physical principles of the SEM and EMP but in XRF analysis the sample is ionized with high energy X-rays instead of accelerated electrons (e.g. Müller, 1972). Analyses were performed at the PetroTectonics analytical facility (Stockholm University).

The local chemical composition (major elements) of micro-scale domains (~ 3.0 x 2.0 mm in size) within micaschists was measured by area scan method at the SEM. The area scan method is used, for example, when modelling compositionally heterogeneous rocks (see section 4.4.3). SEM area scan analyses were performed at the Swedish Museum of Natural History (Stockholm).

The H₂O content of micaschist samples was measured by loss on ignition (LOI) and used to assess hydration (paper II). In LOI analysis, the sample is ignited at 1000 °C for two hours. As a result, the volatiles (e.g. mineral-bound H₂O) are lost and their proportion can be obtained by weight difference before and after ignition.

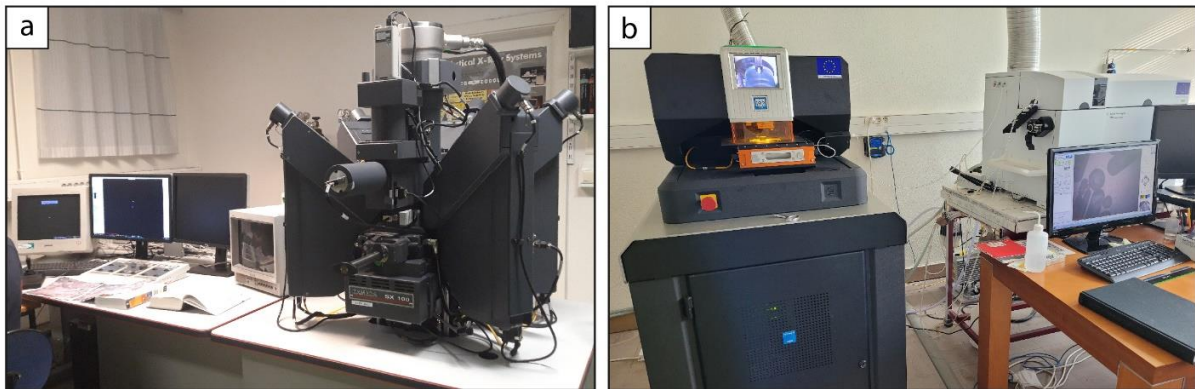


Fig. 3. Analytical setup used. (a) Electron microprobe at the University of Oslo. The central vertical column generates the electron beam and the five inclined columns host the wavelength dispersive spectrometer. (b) Laser-ablation ion-coupled-plasma mass-spectrometer at the University of Rennes. The unit on the left-hand side is the laser-ablation section and the unit on the right-hand side is the ionizer and mass-spectrometer section.

4.4 Thermodynamic modelling

Thermodynamic modelling was used mainly for three purposes: constraining the P – T evolution (papers I and II); reconstructing the H₂O content evolution (paper II); and reconstructing the history of growth and dissolution of key minerals, such as garnet (papers I and II). A few key micaschist samples were selected for thermodynamic modelling (Table 1).

Since the seminal works of Goldschmidt (1912) and Thompson (1955) the principles of thermodynamics have been used to describe metamorphic equilibrium between phases in simple chemical systems of petrologic interest. Today, thanks to the advent of computer modelling and the development of large thermodynamic datasets, we are able to calculate equilibria in complex rock-systems. The dataset contains the thermodynamic properties of the phases, such as Gibbs free energy, enthalpy, entropy, heat capacity and molar volume. The dataset also includes activity-composition models which express the thermodynamic mixing properties of a solid (or fluid) solution phase. Activity-composition models can be determined experimentally (on artificial materials) or empirically (on natural samples). The dataset is internally consistent, which implies that all thermodynamic data taken from different studies are integrated, and that thermodynamic parameters are elaborated with the same methodology.

There are two methods to constrain P – T conditions using thermodynamic modelling: inverse modelling and forward modelling (e.g. Lanari & Duesterhoeft, 2019). Inverse modelling consists in calculating the P – T conditions of equilibration of a mineral assemblage given the measured mineral compositions. Multiple geothermometers and geobarometers can be combined to tightly constrain the P – T conditions of equilibration. This method is referred to as “optimal thermobarometry” or “multi equilibrium thermobarometry” and is commonly performed with the software *average PT*, available within the THERMOCALC package (Powell & Holland, 1994).

Conversely, forward modelling consists in calculating the stable mineral assemblage and mineral compositions given the P – T conditions of interest. The P – T conditions of equilibration are constrained by comparison of the studied sample (mineral assemblage and composition) with the calculated model. In this study we utilized forward modelling because it allowed us to reconstruct not only the P – T evolution but also the history of mineral growth/dissolution and the H_2O content evolution. The software used in this study was Theriak-Domino (De Capitani & Petrakakis, 2010), which utilizes an algorithm to minimize Gibbs free energy in order to generate an isochemical phase diagram.

4.4.1 Isochemical phase diagrams

A phase diagram shows the thermodynamically stable phases within a P – T coordinate system. However, phase stability is not only a function of the P – T conditions, but also of the composition of the system (also referred to as P – T – X conditions). Firstly pioneered by Hensen & Essene (1971) without the use of computer programs and then popularised by Powell et al. (1998), isochemical phase diagrams (or pseudosections) provide a control on the system composition. Isochemical phase diagrams are calculated from a given chemical composition (i.e the bulk-rock composition) representative of a specific sample (or domain). In this study the chemical system considered comprises the following elemental components: MnO, Na₂O, CaO, K₂O, FeO, MgO, Al₂O₃, SiO₂, H₂O, TiO₂, Fe₂O₃ (MnNCKFMASHTO).

An introduction on how to read isochemical phase diagrams is given below. Two isochemical phase diagrams were calculated for two meta-pelites with different bulk-rock compositions (Fig. 4). Sample 1 is poorer in Al₂O₃ with respect to sample 2. Their bulk-rock composition can be plotted on an AFM ternary diagram, using the proportions of FeO, MgO and Al₂O₃ (projected from muscovite). In the isochemical phase diagrams, each line marks the appearance or disappearance of a phase in the stable assemblage. For example, consider the prograde reaction:



In the AFM diagram, this reaction marks the disappearance of the tieline garnet-chlorite and the appearance of the tieline staurolite-biotite. Sample 1, being poorer in Al₂O₃, plots below the tieline garnet-chlorite, whereas sample 2 plots above. In both samples, chlorite is completely consumed

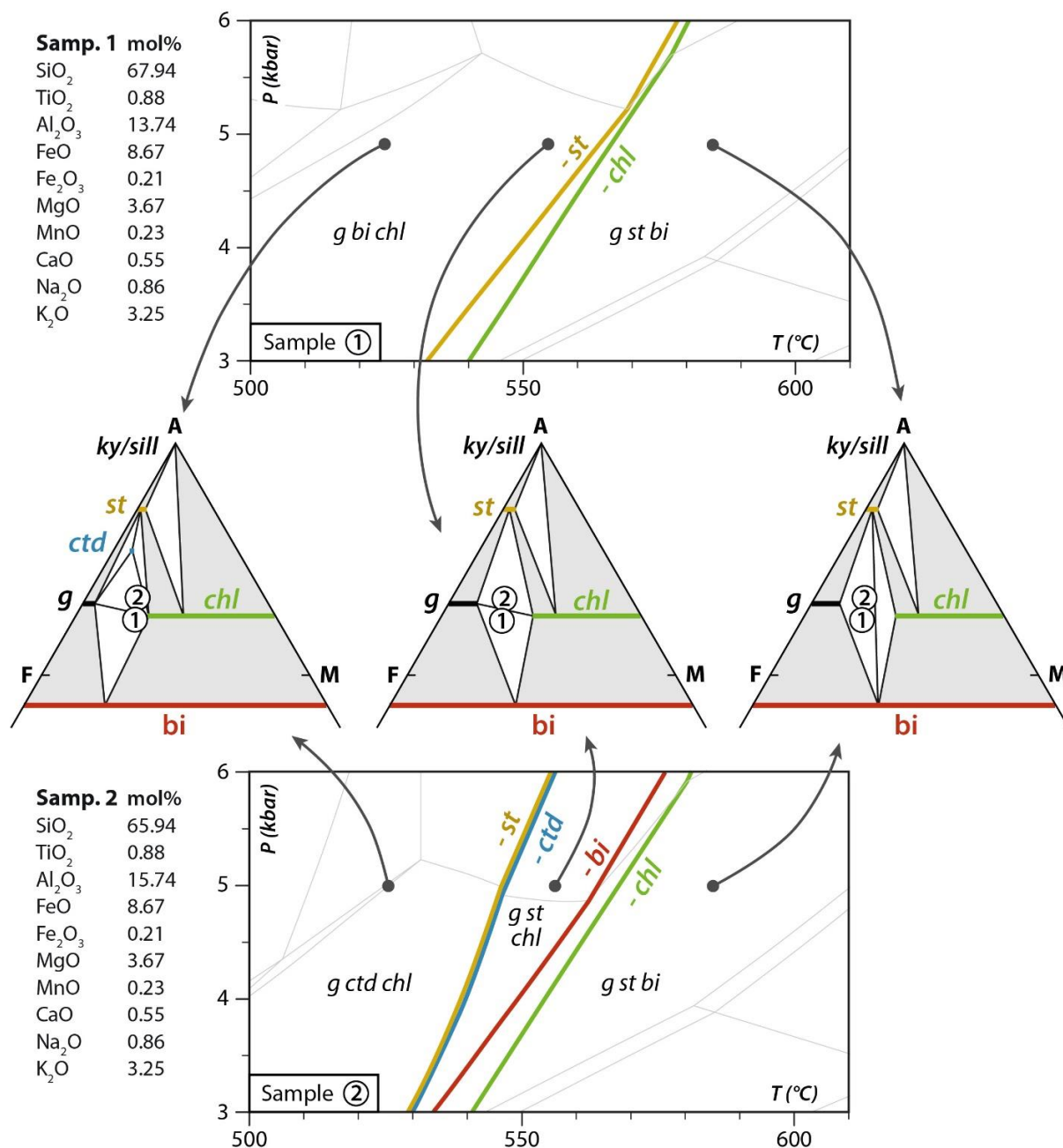


Fig. 4. Examples of isochemical phase diagrams calculated for two different bulk-rock compositions: an Al₂O₃-poor meta-pelite (sample 1) and an Al₂O₃-rich meta-pelite (sample 2). Phase diagrams were calculated with Theriak-Domino in the system MnNCKFMASHTO, considering excess H₂O. The boundaries of the stability fields are indicated with thick colored lines for minerals of interest, and with thin grey lines for other minerals. Only the minerals of interests (g = garnet, st = staurolite, ctd = chloritoid, bi = biotite, chl = chlorite) are reported in the stable mineral assemblages, although other minerals can also be present. Qualitative AFM ternary diagrams are given at three different *P*-*T* conditions, before and after the occurrence of major metamorphic reactions.

during this reaction and disappears from the stable assemblage. However, the reaction marks the first appearance of two different minerals in the two samples, namely staurolite in sample 1 and biotite in sample 2. In fact, in sample 2 staurolite was already present in the system before the reaction occurs, as a result of the break-down of chloritoid at lower T .

The phase diagram can be contoured with isolines that show the variation of a quantity of interest, such as mineral composition (isopleths), mineral modal proportion (isomodes) and H_2O content.

4.4.2 H_2O conditions and T - $M(H_2O)$ diagrams

In isochemical phase diagrams, H_2O is treated as a chemical component of the system, likewise e.g. SiO_2 or Al_2O_3 . The bulk H_2O content represents the available amount of H_2O in the rock-system and is hereafter referred to as $M(H_2O)$. When the software calculates the stable assemblage, it distributes the H_2O among the stable hydrous minerals (as H_2O bounded to the mineral crystal lattice). If $M(H_2O)$ is too low to satisfy the demand of mineral-bound H_2O in hydrous minerals, anhydrous minerals are stabilized instead. This condition is referred to as H_2O -undersaturation. If H_2O remains in excess after having been distributed among hydrous minerals, it forms a separate fluid phase (or “free H_2O ”) that fills the intergranular space. In thermodynamic modelling, when free H_2O is present, the system is considered H_2O -saturated. The concept is analogous to that of SiO_2 -saturation, common in most meta-pelite compositions. In SiO_2 -saturated rocks, the excess SiO_2 that remains in the system after partitioning in silicates forms a separate SiO_2 phase (i.e. quartz). Because anhydrous minerals are preferentially stabilized at higher T (see section 1.6), phase diagrams may contain a H_2O -saturation limit that divides the P - T space into a H_2O -saturated field at higher T and a H_2O -undersaturated field at lower T .

To investigate the influence of H_2O availability on the stability of mineral assemblages and mineral compositions, T - $M(H_2O)$ diagrams were calculated (e.g. Fig. 11). In these diagrams, $M(H_2O)$ varies along the x-axis and T varies along the y-axis, while P is kept constant. The H_2O -saturated field occurs on the right-hand side of the diagram, at high $M(H_2O)$ and high T . At $M(H_2O) = 0$ the stable mineral assemblage consists entirely of anhydrous minerals. In this study, the fluid was always assumed to be pure H_2O because carbonate (mineral-bound CO_2) is not present in the studied micaschists.

4.4.3 Limitations and corrections

Thermodynamic modelling is currently the most reliable method to constrain P - T conditions, although it is affected by considerable limitations. The choice of the thermodynamic dataset, among those available in the literature, can affect the topology of the calculated diagrams. The robustness of the thermodynamic dataset strictly depends on the availability of systematic

thermodynamic data and on the accuracy of the solid solution models. Throughout this study the dataset 5.5 of Holland & Powell (1998; converted for Theriak-Domino by D. K. Tinkham) was used.

Thermodynamic modelling assumes that perfect equilibrium was achieved in the rock-system. However, natural metamorphic rocks are archives of disequilibrium textures. For example, equilibration may be attained locally in discrete volumes. This is mainly the result of sluggish diffusivity of chemical components through the intergranular medium, which limits the volume of equilibration (e.g. Carlson, 2002; Carlson et al., 2015). The preservation of incomplete reaction textures, metastable relicts and compositional zonings (e.g. in garnet) testifies that disequilibrium at the crystal-scale persists despite metamorphic overprint. During growth, garnet sequesters chemical components (mainly Mn, Fe, Ca and Al) within its core in a process called garnet fractionation (Hollister, 1966; Evans, 2004; Gaidies et al., 2006). Those elements are effectively shielded from the rest of the rock. As a result, the matrix is progressively depleted of chemical components during garnet growth. This is particularly evident in polycyclic rocks.

To address these issues, the bulk-rock composition was carefully assessed and re-assessed for each studied sample at different steps of their polycyclic evolution. The studied polycyclic micaschists often display compositional heterogeneities, such as alternation of layers with different mineral modal proportions, and exhibit relicts of a first metamorphic cycle. Therefore, isochemical phase diagrams were preferentially calculated considering the composition of a local volume of equilibration (measured by SEM area scan). To correct for garnet fractionation, representative chemical analyses of garnet (obtained by EMP or SEM area scan) were subtracted from the bulk-rock composition in proportion to the garnet modal amount. Alternatively, garnet fractionation was corrected by excluding specific garnet zones from the analysed local area (at the SEM).

The following further corrections were applied to the bulk-rock composition used in the calculations. Ferric and ferrous iron are not differentiated in the bulk-rock analyses. Ferric iron content was assumed to be low and set to 5 wt.% of the total iron. Phosphorous is not considered as a chemical component of the system because systematic thermodynamic data and solid-solution models of phosphates are lacking. However, the calcium content in the bulk-rock composition may be overestimated if a Ca-rich phosphate (mainly apatite) is present in the analysed rock volume. Therefore, the bulk calcium content was corrected using the measured amount of phosphorous, according to the proportion of calcium in apatite.

4.5 Geochronology and trace element geochemistry

U-(Th)-Pb geochronology was conducted on selected orthogneiss (using zircon) and micaschist samples (using zircon and monazite; Table 1). The aim was twofold: to determine the age of the protolith (age of magmatism and maximum deposition age of sediments; papers I and III) and to constrain the age of metamorphic events (paper I).

4.5.1 U-(Th)-Pb dating

The absolute age of a geologic event can be determined by exploiting the natural phenomenon of radioactive decay (firstly detected by Becquerel, 1896, and Curie & Sklodowska-Curie, 1898, on U materials). This consists in the spontaneous transformation of an unstable parent isotope into a stable daughter isotope. Isotope stability results from the balance of the attractive strong nuclear force and the repulsive electromagnetic force acting between the particles that compose the atomic nucleus (protons and neutrons). In general, the strong nuclear force prevails in small and light isotopes whereas the electromagnetic force tends to destabilize large and heavy isotopes (such as the isotopes of U). To restore equilibrium, heavy parent isotopes eject particles and decay into lighter daughter isotopes. Conveniently, radioactive decay occurs at a constant rate for each parent-daughter system and is quantified by the decay constant λ . Therefore, the time passed since the closure of the isotopic system (t) is directly proportional to the ratio of the amount of daughter isotope over the amount of parent isotope, according to the equation:

$$t = \frac{1}{\lambda} \ln \left(\frac{\text{"daughter"}}{\text{"parent"}} + 1 \right)$$

Closure of the isotopic system is achieved when the system (e.g. a crystal containing radioactive isotopes) stops exchanging isotopes with its environment. This occurs below a specific T (i.e. the closure temperature, T_c) for each mineral species and for each parent-daughter system. U-Th-Pb dating is based on the decay of the parent isotopes ^{238}U , ^{235}U and ^{232}Th into the respective daughter isotopes ^{206}Pb , ^{207}Pb and ^{208}Pb , with several intermediate steps.

Zircon (ZrSiO_4) is the archetypal geochronometer, whose potential was recognized already by Holmes (1911). During zircon growth, U^{4+} can substitute Zr^{4+} in the crystal lattice and reach up to thousands of ppm in concentrations, whereas Pb is generally not incorporated (Watson et al., 1997; Hoskin & Schaltegger, 2003). This implies that virtually all the Pb contained in zircon at any given time is radiogenic (i.e. derives from radioactive decay) and the initial non-radiogenic Pb (present in the crystal at $t = 0$) can be assumed to be negligible. Th in zircon is generally too low to be used for geochronology. Zircon is a very common accessory mineral in felsic magmatic rocks, in metamorphic rocks and as a detrital mineral in sedimentary rocks. Thanks to its mechanical and chemical resilience, zircon can withstand processes such as partial melting, metamorphism and transport within sediments, acting as a time capsule for the oldest geologic history.

Monazite ($(\text{LREE})\text{PO}_4$) has been used as a geochronometer in more recent times (Parrish, 1990). It can incorporate U in concentrations of a few wt.% and Th in several wt.%, whereas non-radiogenic Pb is generally (but not always) low. Monazite mainly occurs in felsic magmatic rocks and in *HT* metamorphic rocks, where it usually grows by consumption of allanite and apatite (Engi, 2017, and references therein). Both zircon and monazite have a T_c (~ 900 °C and ~ 725 °C, respectively; Cheriak & Watson, 2001; Parrish, 1990) generally higher than the T at which they

commonly form in magmatic and metamorphic environments. This implies that U-(Th)-Pb dating provides the timing of mineral growth.

A key advantage of U-(Th)-Pb dating is that independent dates from distinct parent-daughter systems can be compared in order to assess accuracy and geologic significance. This can be done by plotting isotopic ratios in a concordia diagram. The most popular concordia diagram is the Wetherill diagram (Wetherill, 1956), which uses the $^{207}\text{Pb}/^{235}\text{U}$ ratio on the x-axis and the $^{206}\text{Pb}/^{238}\text{U}$ on the y-axis (e.g. Fig. 9b, e). The concordia line is the locus of points where the isotopic ratios of the two isotopic systems yield the same date. If measured ratios plot on the concordia line, they are considered to be concordant and the resulting age likely has geological significance. In the Wetherill concordia diagram, discordance is mainly attributed either to (i) Pb loss or (ii) mixing. (i) Part of the radiogenic Pb may be lost if the isotopic system is partially re-opened, for example during metamorphism or recent weathering. Pb loss may occur by diffusion through the crystal lattice, although some authors have pointed out that Pb diffusion in non-metamictic zircon is negligible at $T < 750\text{ }^{\circ}\text{C}$ (Cherniak & Watson, 2001; Villa & Hanchar, 2017). (ii) Mineral geochronometers, such as zircon, commonly display complex internal textures, with multiples shells of growth and overgrowths added throughout their geologic history. A measurement of the isotopic content of mixed growth zones provides mixed ages. The strength of concordia diagrams is that discordance can still provide geologically meaningful results if discordant data define a line (i.e. discordia line). The upper and lower intercept of the discordia line with the concordia line represent the age of the early event (such as crystallization of the magmatic zircon core) and the younger event (such as metamorphic Pb loss or overgrowth), respectively.

When dealing with large datasets, data are treated with statistical methods. Hereafter the term “date” is used to indicate an age calculated from a single measured isotopic ratio, whereas the term “age” is derived from a statistically-significant dataset. The concordia age is a weighted mean which considers the analytical uncertainties and the concordance of every single isotopic ratio (Ludwig, 1998). With the concordia age, an error (in this study given as 95% confidence interval) and a mean squared weighted deviation (MSWD) are calculated. The MSWD (concordance + equivalence) is a statistical parameter that is used firstly to test concordance and secondly to assess the assumption that the scatter of data is the result of analytical uncertainties (repeated measurements of the same point) and not of mixing of two or more geologically meaningful ages. For optimal concordance and equivalence the MSWD should be around 1.

4.5.2 Protolith age of meta-sediments: detrital zircon

The age of a sediment is typically determined using the fossil record. However, the latter is generally lost during metamorphic recrystallization and deformation. A first approach to approximate the protolith age of a meta-sediment is to correlate it with stratigraphic successions of well-known age, on the basis of the lithological and paleogeographic affinity. This method can provide robust and precise age estimations only when diagnostic sedimentary features (e.g.

sedimentary structures, conglomerate layers, ankerite layers, brecciated carbonates) are identified, despite the metamorphic overprint.

A different approach is to bracket the age of sedimentation within a time interval, using radiometric dating. The upper age limit of sedimentation (minimum deposition age) may be provided by the age of intrusion of a magmatic body within the sediment or by the age of a metamorphic overprint. The lower age limit (maximum deposition age) can be constrained by detrital zircon (e.g. Fedo et al., 2003). Detrital zircon geochronology consists in dating zircon crystals that were eroded from a source rock and deposited with the sediment. Detrital zircon can withstand subsequent metamorphism and retain the age signal of the sediment source rocks. The age of sedimentation must be younger than the age of the youngest detrital zircon. Detrital zircon can also be used to constrain the provenance of the sediments, with implications for paleogeographic reconstructions.

A robust detrital zircon study, in particular if used for provenance, requires statistical treatment of the detrital zircon age distribution (Andersen, 2005; Malusà et al., 2013). A minimum of 117 crystals should be analysed in order to ensure detection (at 95% confidence level) of every age population in a sample (Vermeesch, 2004). Provenance studies were out of the scope of the present study, and detrital zircons were used exclusively to constrain the maximum age of deposition of meta-sediments. Due to the small size of detrital zircons in the studied micaschist samples, it was not possible to obtain a statistically significant number of measurements. Nonetheless the obtained data can be used as a qualitative indication of the maximum age of sedimentation (paper I).

4.5.3 *Interpreting metamorphic ages: petrochronology*

Deciphering the geologic significance of the obtained metamorphic ages is often challenging. In fact, metamorphism is not an instantaneous event but occurs over a P - T cycle. While P - T estimates are based on thermodynamics of rock-forming minerals (e.g. garnet, chloritoid, muscovite), the timing is constrained using accessory minerals (e.g. zircon, monazite). Unfortunately, systematic thermodynamic data for accessory minerals are still lacking and, thus, we are not yet able to model their history of growth and dissolution throughout the P - T evolution. In order to reconstruct the P - T - t path, where pressure, temperature and time are linked, the interplay of growth and dissolution between rock-forming minerals and accessory minerals has to be unfolded. This has been recently defined as a new discipline and named petrochronology (e.g. Engi et al., 2017).

In this study, the coexistence of rock-forming minerals and accessory minerals was firstly assessed by investigating their microtextural relationships in thin section (e.g. monazite and apatite inclusions in garnet). Measurement of the trace element content was also used to assess chemical equilibrium. For example, garnet is known to uptake a large portion of a rock's HREE budget (Otamendi et al 2002; Gaidies, et al., 2020). Therefore, metamorphic zircon growing in presence of garnet is expected to be depleted in HREE and will exhibit a flat HREE pattern (Rubatto, 2002;

Rubatto, 2017). By contrast, zircon growing in absence of garnet, or during garnet consumption, will display a HREE pattern with a positive slope.

4.5.4 Laser-ablation ion-coupled-plasma mass-spectrometry (LA-ICP-MS)

Monazite was analysed in thin section whereas zircon was extracted from the hand sample and analysed on prepared mounts. Zircons were separated hydrodynamically from crushed hand sample powder using a Wilfley Table. The latter is designed to facilitate grain sorting in a water current, exploiting the density contrast between heavy zircons and the rest of the light mineral fraction. Zircons contained in the concentrate were handpicked and mounted on epoxy resin pucks (mounts). The internal zoning of zircon and monazite was studied at the SEM by cathodoluminescence (CL) and BSE imaging, respectively. Zircon and monazite were analysed by Laser-ablation ion-coupled-plasma mass-spectrometry (LA-ICP-MS).

LA-ICP-MS is an analytical technique used to determine elemental and isotopic composition even in very low concentrations (detection limit for most species of 0.01 ppm). The technique started to develop in the 90's (e.g. Fryer et al., 1993; Hirata & Nesbitt, 1995) and is now broadly used in U-(Th)-Pb dating and trace element analysis, mainly thanks to its low operation cost, its simple and fast sample preparation and analysis and its decent precision. The instrument is composed of three sectors (Fig. 3b). The laser-ablation sector (LA) is responsible for extraction of the material from the sample. A high intensity laser (usually in the ultraviolet energy range) is shot in high frequency pulses on the surface of the sample, inducing a so-called sample "ablation": a mixture of physical processes such as photoionization, volatilization and melt extraction. Specific growth zones within the analysed mineral (e.g. the detrital core or the metamorphic rim of zircon) can be targeted. The size of the ablation area (the spot diameter) can be chosen in function of the thickness of the growth zone of interest, the element concentration in the analysed mineral and the desired analytical precision. The ablated material is taken in charge by a flow of carrier gas (usually an unreactive noble gas such as Ar) and transported to the next sectors. In the ion-coupled-plasma (ICP) sector, the ablated material is completely vaporized and ionized at very high temperatures using an induction coil. The elemental and isotopic concentrations are then measured in the mass-spectrometer (MS) sector. For this study a single collector quadrupole mass-spectrometer was utilized. The quadrupole consists of four metal rods which generate an electro-magnetic field. The electro-magnetic field deflects the trajectory of ions depending on their mass to charge ratio. By quickly adjusting the current inside the rods, specific isotopes of interest are sent to the detector whereas others are dispersed. Finally, the detector counts the number of ions received. Quantification of the isotopic concentration is done by calibration respect to a primary standard material, whose composition is well-known. A secondary standard of known composition is used to control precision and accuracy of the results. During the analytical session, measurements of the unknown (the sample) are bracketed between repeated measurements of the primary and secondary standards.

5. Results and interpretations

5.1 Geology of the northern Dora-Maira Massif: lithologies, age of the protoliths and tectonic architecture (papers I and III)

Detailed field work along the transect offered by the Chisone Valley and Germanasca Valley allowed to redefine the tectonic architecture of the northern Dora-Maira Massif. We identified four tectonic units which differ for lithologies, age of the protoliths, and Alpine peak P - T conditions. The units are separated by tectonic boundaries. In the northern Dora-Maira Massif the following tectonic units are stacked from bottom to top: the Pinerolo Unit, the Chasteiran Unit, the Muret Unit, the Serre Unit (Fig. 5).

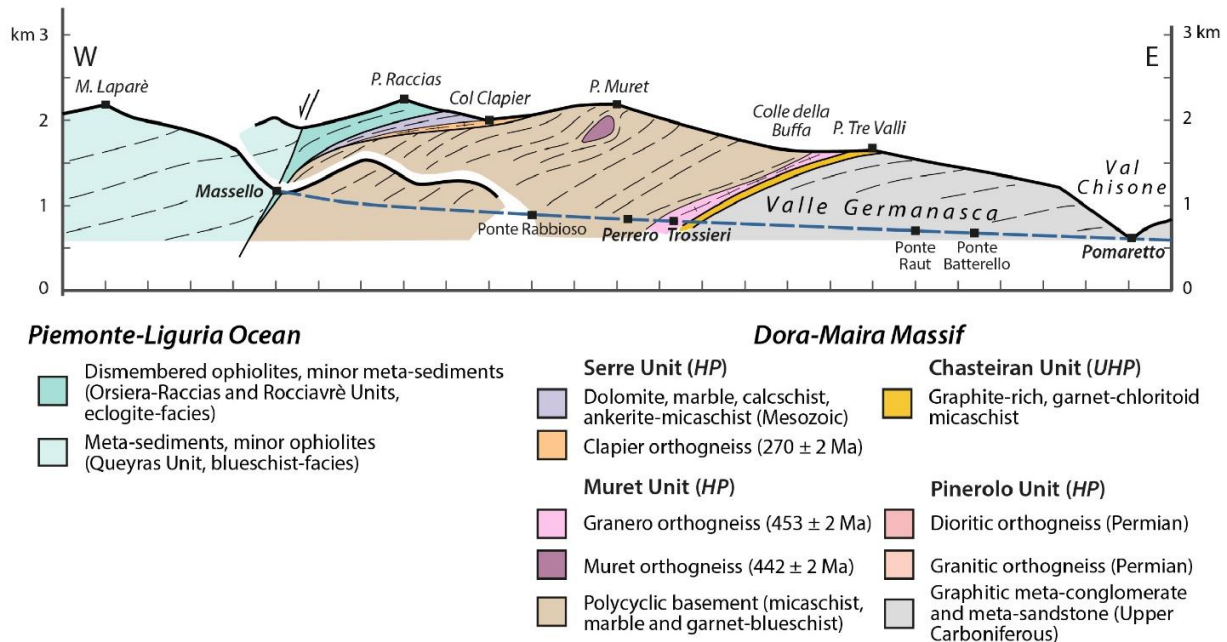


Fig. 5. Cross section across the Germanasca Valley, showing the stack of tectonic units in the northern Dora-Maira Massif. Modified from Manzotti et al. (2022) and taken from paper III.

5.1.1 Pinerolo Unit

The Pinerolo Unit is characterized by Upper Carboniferous meta-sediments, whose age of deposition is bracketed by the age of the youngest detrital zircon (~ 330 Ma; Manzotti et al., 2016) and the age of intrusion of granitic and dioritic bodies (304–268 Ma; Bussy & Cadoppi, 1996). Despite the intense Alpine deformation and metamorphism, we were able to identify some primary

sedimentary features and structures. Typical of the Pinerolo Unit are cyclic successions of interbedded meta-conglomerates, meta-sandstones with locally preserved cross-bedding lamination, and graphite-rich meta-mudstones. We interpreted these as fluvial, flood plain and lacustrine deposits with local intense accumulation of organic matter, similarly to other non-metamorphosed Upper Carboniferous successions in the Alps (e.g. in the Zone Houlliere; Fig. 2; Manzotti et al., 2016) and elsewhere (e.g. Fielding, 2021).

5.1.2 Chasteiran Unit

The Chasteiran Unit is a thin (a few tens of metres thick) but continuous unit consisting of graphite-rich garnet-chloritoid mylonitic micaschists. In these rocks coesite was found as inclusions within garnet, indicating *UHP* Alpine conditions (Manzotti et al., 2022). The Chasteiran Unit differs from the Pinerolo unit for Alpine *P–T* conditions and lithology. In agreement with Manzotti et al. (2022) we propose that the graphite-rich micaschists from the Chasteiran Unit do not derive from a Carboniferous protolith (as previously assumed) but from black shales of Silurian age because a similar lithology occurs in the polycyclic basement (see section 5.1.3), in correlation with non-metamorphosed successions of Lower Palaeozoic age found elsewhere (e.g. in Sardinia; Cocco et al., 2018).

5.1.3 Muret Unit

The Muret Unit mainly consists of a polycyclic basement, comprising garnet-chloritoid micaschists and minor paragneisses, orthogneisses, meta-basites and marbles. Most of these lithologies display relicts of a pre-Alpine (Variscan) metamorphic cycle that we characterized for *P–T* evolution and timing in paper I (see section 5.4). In contrast with the Chasteiran Unit, the Alpine peak *P–T* conditions in the Muret Unit, estimated in paper II (see section 5.5), did not reach the coesite stability field.

Orthogneisses are found in a hectometre-thick layer at the base of the Muret Unit (named Granero orthogneiss) or is a hectometre-scale body intruded within the micaschists (named Muret orthogneiss). The Granero orthogneiss is strongly mylonitic and, thus, is considered the marker of the tectonic boundary with the Chasteiran Unit. We dated the two orthogneisses and established the Upper Ordovician to Early Silurian age of their magmatic protolith (460–442 Ma), partly disproving previous assumptions.

The protolith age of the micaschists intruded by the Muret orthogneiss (referred to as garnet-staurolite micaschists because of their noticeable pre-Alpine relicts) is bracketed between the Cambrian and the Ordovician by the youngest detrital zircon (~ 590 Ma) and the age of the Muret orthogneiss. In other graphite-rich garnet-chloritoid micaschists, the youngest detrital zircon (~ 450 Ma) suggests a Silurian to Devonian protolith age.

5.1.4 Serre Unit

The tectonic boundary between the Muret Unit and the Serre Unit is marked by a ductile shear zone with tectonic slices of serpentine schists and other lithologies. The ductile shear zone is locally overprinted by a cataclastic shear zone cross-cutting the foliation in the Muret Unit. The Serre Unit comprises metre to hectometre-scale tectonic slices of felsic orthogneisses (named Clavier orthogneiss), monocyclic micaschists often ankerite-bearing, dolostones, marbles and calcschists. We dated the Clavier orthogneiss and obtained a Permian age for its magmatic protolith (~ 270 Ma). We interpret the orthogneisses and the associated micaschists as a volcanic or volcanoclastic succession, in agreement with previous authors (Vialon, 1966). The carbonate-bearing rocks represent rests of dismembered Mesozoic covers, in correlation with better preserved successions in the Briançonnais (e.g. Michard et al., 2022).

5.2 Petrology of weakly and strongly reworked polycyclic rocks (papers I and II)

The pre-Alpine basement found in the Muret Unit was strongly reworked during the Alpine metamorphic overprint and deformation. However, we discovered a kilometre-scale domain little affected by the Alpine deformation, enclosed within strongly deformed material. Here, pre-Alpine structures and minerals partly survived, providing an exceptional window into the former orogenic cycle. This is hereafter referred to as the low-strain (Alpine) domain, although rocks in it were strongly deformed during the pre-Alpine cycle. The Muret orthogneiss forms the core of the low-strain domain, whereas in the surrounding micaschists, the Alpine deformation progressively increases moving further away from the orthogneiss body.

Within the low-strain domain, orthogneisses and micaschists preserve a pre-Alpine *HT-LP* foliation (Fig. 6). The latter is defined by low-Si muscovite ($\text{Si} \approx 3.2$ atoms per formula unit, a.p.f.u.) and Ti-rich biotite in orthogneiss and by relict low-Si muscovite cores ($\text{Si} \approx 3.1$ a.p.f.u.) in micaschist. Centimetre-sized prismatic-shaped pseudomorphs after staurolite are oriented parallel to the pre-Alpine foliation in micaschists. Pre-Alpine garnet is preserved in both orthogneisses and micaschists. In micaschists outside the low-strain domain (in high-strain domains) staurolite pseudomorphs are absent and the only pre-Alpine relicts are a first generation of garnet and its inclusions.

The Alpine *HP* overprint in the Muret orthogneiss is essentially absent, whereas in micaschists (in both low- and high-strain domains) it is characterized by the assemblage garnet, high-Si muscovite ($\text{Si} \approx 3.4\text{--}3.5$ a.p.f.u.), chloritoid, glaucophane (pseudomorphed during late Alpine retrogression) and rutile. In micaschists from the low-strain domain the Alpine minerals grow statically over the pre-Alpine foliation. High-Si muscovite concentrically overgrows low-Si muscovite. A fine-grained aggregate of Alpine chloritoid surrounded by a corona of Alpine high-Si muscovite replaces the original pre-Alpine staurolite. By contrast, micaschists in high-strain

domains display a fully recrystallized Alpine *HP* foliation defined by high-Si muscovite and chloritoid.

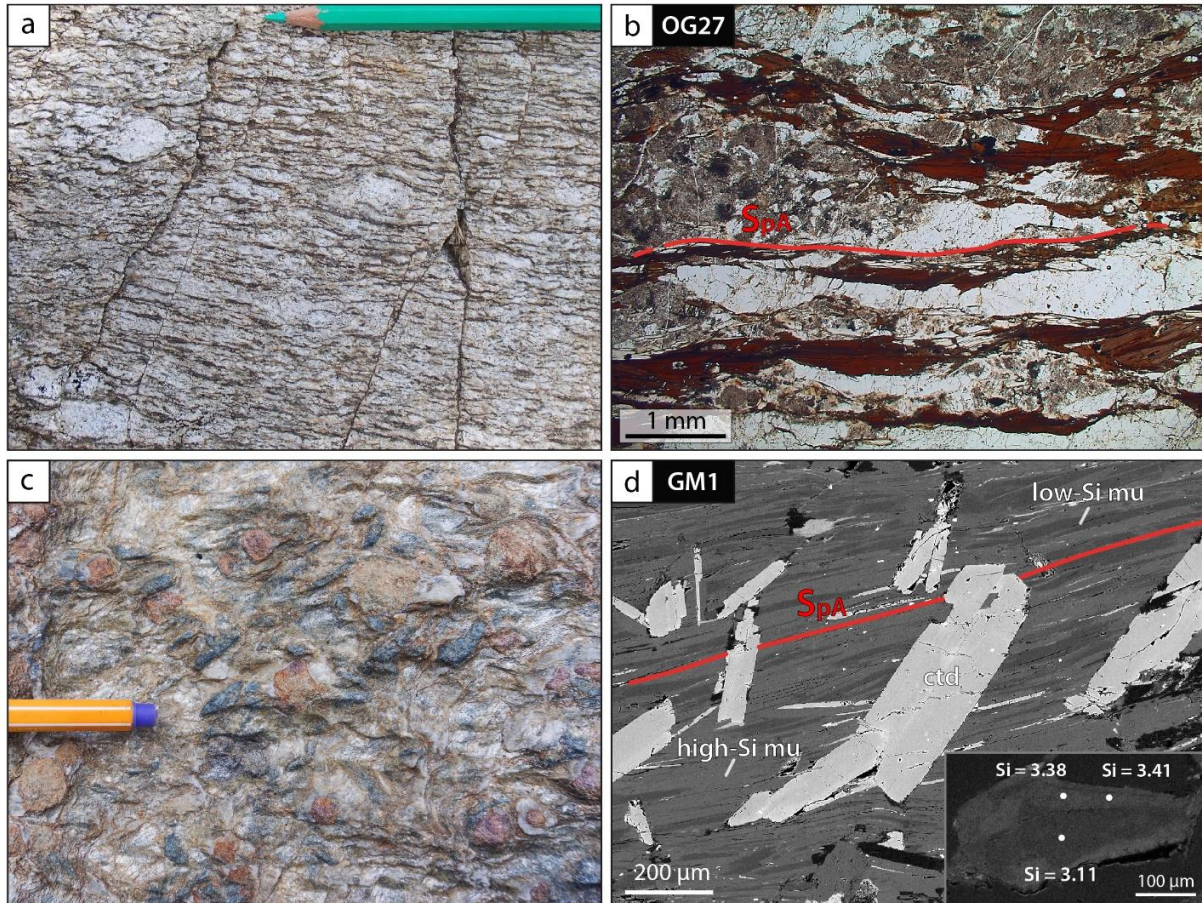


Fig. 6. Lithologies within low-strain domain. (a) Field aspect of Muret orthogneiss (from paper I; Nosenzo et al., 2022). (b) Plane polarized light (PPL) photomicrograph of Muret orthogneiss with a pre-Alpine foliation (SpA) defined by Ti-rich biotite and low-Si muscovite. (c) Field aspect of micaschists with centimetre-scale porphyroblasts of polycyclic garnet and pseudomorphed pre-Alpine staurolite. (d) Backscattered electron (BSE) images of micaschist with a pre-Alpine foliation (SpA) defined by pre-Alpine low-Si muscovite (darker BSE emission; mu). Alpine high-Si muscovite (brighter BSE emission) concentrically overgrows and replaces low-Si muscovite. Alpine chloritoid (ctd) is post-kinematic respect to the pre-Alpine foliation.

5.3 Polycyclic garnet textures (papers I and II)

We studied in detail garnet from both weakly and strongly re-deformed micaschists because it records exceptionally well the polycyclic evolution. In low- and high-strain domains, garnet records the same polycyclic P - T -fluid evolution although the textures are different, mostly reflecting differences in initial bulk-rock composition of the micaschists in the two domains and different pre-Alpine garnet size. We will hereafter describe garnet in the micaschists from the low-strain domain only, because it exhibits the most compelling textures. Garnet is polycyclic, which is to say that it comprises a first generation of pre-Alpine age and a second generation of Alpine age (Fig. 7).

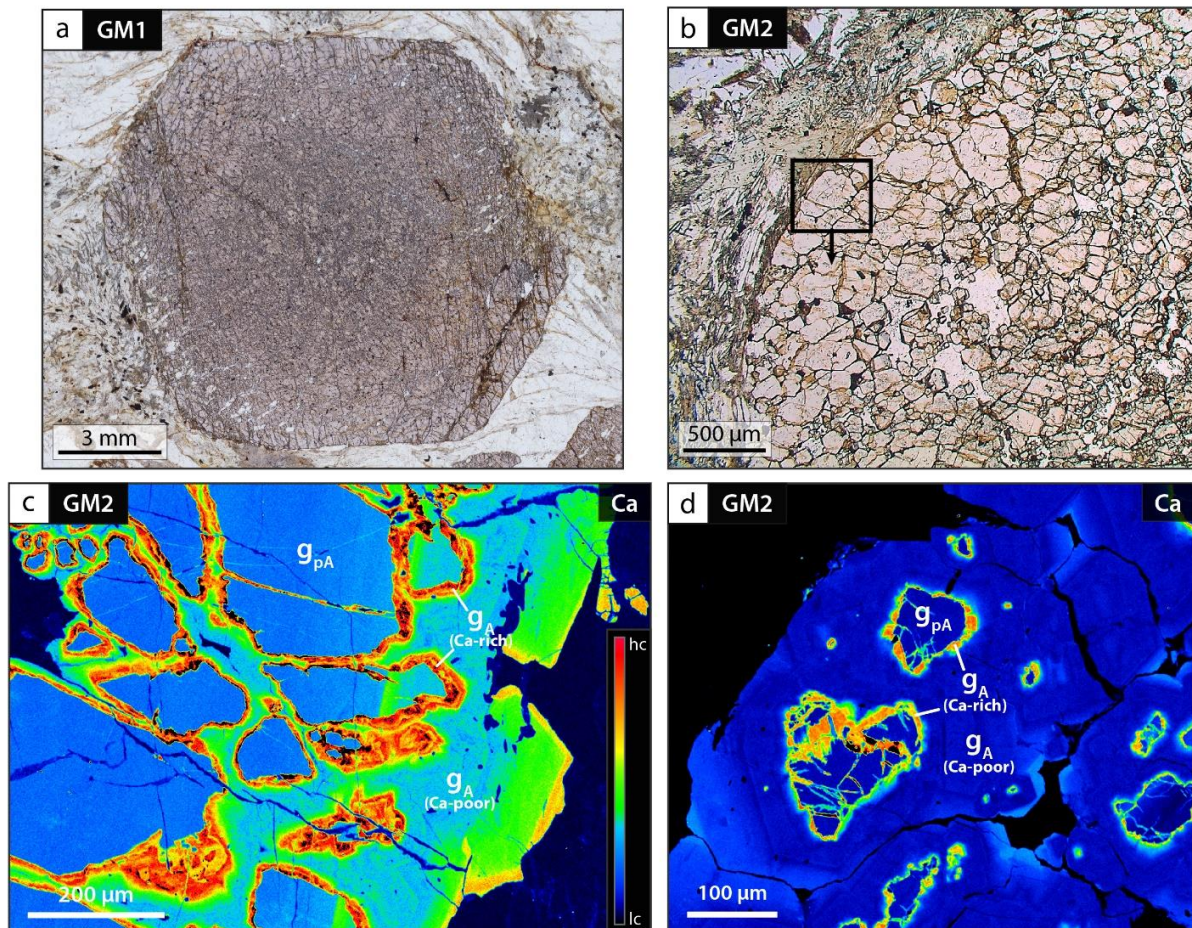


Fig. 7. Polycyclic garnet textures. (a) PPL photomicrograph of euhedral porphyroblastic garnet. (b) Detail of the outer portion of a porphyroblast. The black square indicates the position of the X-ray map in (d). (c, d) X-ray maps of Ca at the outer portion of a porphyroblast. Pre-Alpine garnet (g_{pA}) is fractured and dissolved. Alpine garnet (g_A) overgrows fragments of pre-Alpine garnet and seals the fractures. Alpine garnet comprises a Ca-rich inner portion and a Ca-poor outer portion. “hc” = high concentration; “lc” = low concentration. Modified from paper II.

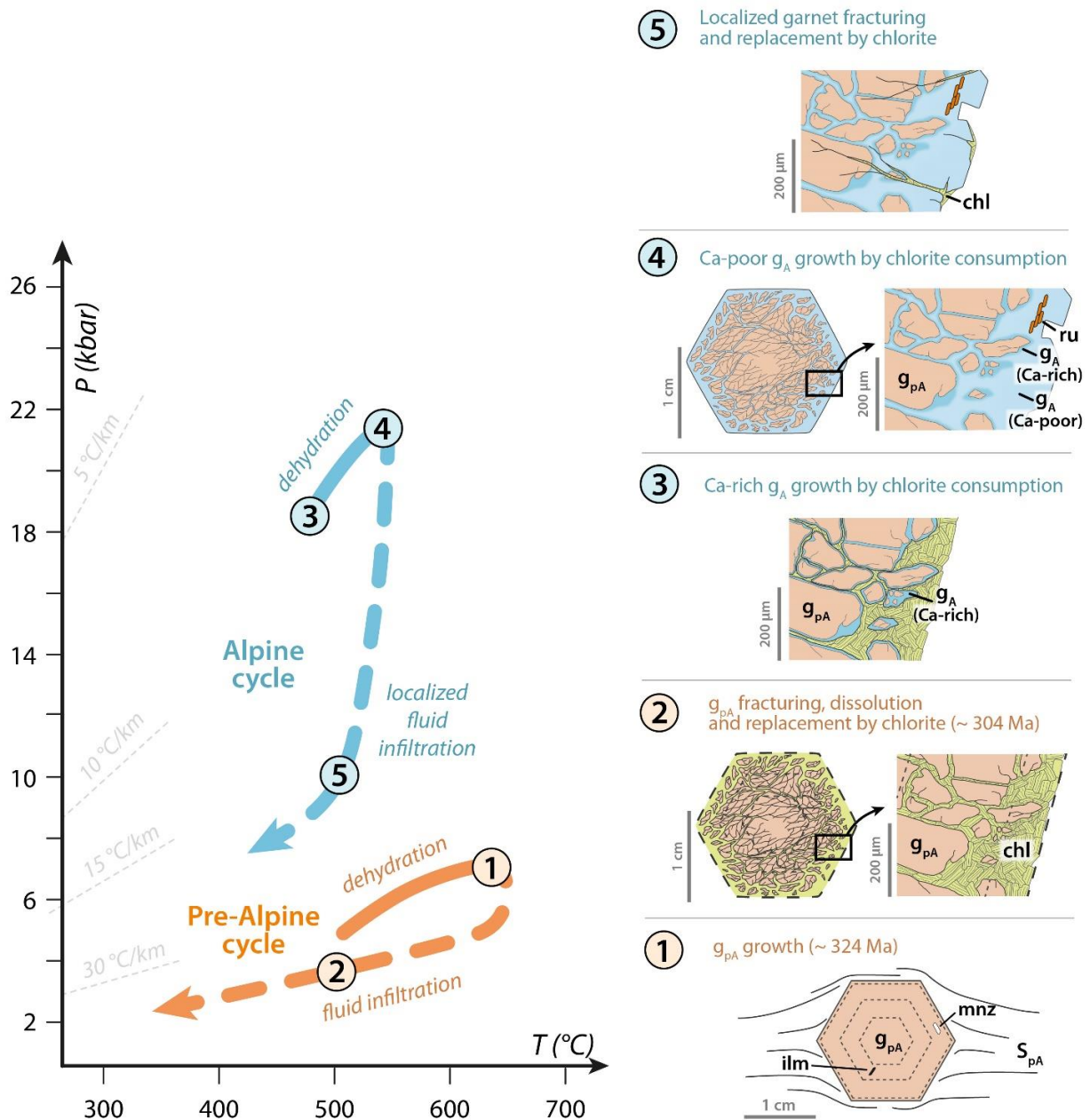


Fig. 8. Polycyclic P - T path of the Muret unit and schematic stages of garnet growth and dissolution associated with fluid evolution in micaschists from the low-strain domain (g_{pA} = pre-Alpine garnet; g_A = Alpine garnet). Chlorite = chl; rutile = ru; monazite = mnz; ilmenite = ilm. Redrawn from paper II.

The first garnet generation forms centimetre-sized porphyroblasts generally wrapped by the pre-Alpine foliation. It includes ilmenite and pseudomorphed staurolite and displays a prograde growth zoning characterized by a decrease in Ca, a bell-shaped decrease in Mn and an increase in Fe and Mg from core to rim. Thermodynamic modelling and geochronology confirm that the first

garnet generation is pre-Alpine and grew along a prograde path up to the amphibolite-facies (see section 5.4; stage 1 in Fig. 8).

Pre-Alpine garnet porphyroblasts are highly fractured and dissolved (Fig. 7c, d). At the rim of the porphyroblasts, where dissolution was more intense, only relict angular and irregularly-shaped pre-Alpine garnet fragments are preserved. Towards the core of the porphyroblasts, pre-Alpine garnet dissolution is concentrated along a network of fractures, recalling a typical “mesh” texture. Pre-Alpine garnet displays embayments along the dissolved edges. Such textures are interpreted as the result of a stage of pseudomorphic replacement of pre-Alpine garnet by chlorite at greenschist-facies conditions (stage 2 in Fig. 8), as documented in garnet of similar age in the Central Alps (Floess & Baumgartner, 2013) and in numerous other cases worldwide (e.g. Prior, 1993). Garnet chloritization was accompanied by fluid infiltration and hydration (see section 5.6).

A second garnet generation, Alpine in age, forms overgrowths (up to 400 μm thick) on partially dissolved pre-Alpine garnet, sealing the space between garnet fragments (Fig. 7 c, d). The final shape of the polycyclic garnet (after pre-Alpine garnet dissolution and Alpine garnet growth) mimics the euhedral shape of the original pre-Alpine porphyroblast (Fig. 7a). This may suggest that Alpine garnet grew by consumption of chlorite (which in turn had previously pseudomorphed pre-Alpine garnet) with preservation of shape. Alpine garnet includes rutile, locally in elongated aggregates likely the product of transformation of original pre-Alpine ilmenite. Alpine garnet displays a continuous prograde growth zoning, generally characterized by a Ca-rich inner portion (stage 3 in Fig. 8) and a Ca-poor outer portion (stage 4 in Fig. 8). Thermodynamic modelling confirms that the second garnet generation grew along the prograde to peak Alpine *HP-LT* evolution (see section 5.5). A second generation of fractures, locally filled with chlorite, crosscuts both pre-Alpine and Alpine garnet, and likely developed during late-Alpine decompression (stage 5 in Fig. 8).

5.4 P–T conditions and timing of the pre-Alpine cycle (paper I)

Preservation of pre-Alpine chemical and isotopic records in the low-strain domain (Muret Unit) provides a unique opportunity to characterize the pre-Alpine metamorphic cycle.

We used thermodynamic modelling and phase diagram calculation on garnet micaschists from both low- and high-strain domains to reconstruct their pre-Alpine *P–T* evolution. Pre-Alpine garnet in the studied micaschist samples grew along the same prograde *P–T* path from 3–6 kbar and 490–540 °C to 6–8 kbar and 640–660 °C. The inferred peak *P–T* conditions (~ 7 kbar and ~ 650 °C) do not exceed the amphibolite-facies, consistently with (i) the presence of pseudomorphs after staurolite and the lack of sillimanite, (ii) the absence of evidence for partial melting (e.g. leucosomes and paleosomes) and (iii) the preservation of the garnet growth zoning, indicating that intracrystalline diffusion was too sluggish to homogenize the internal composition of garnet (e.g. Caddick et al., 2010; Ganguly, 2010). These results are in agreement with Cadoppi (1990) and disprove Bouffete et al. (1993).

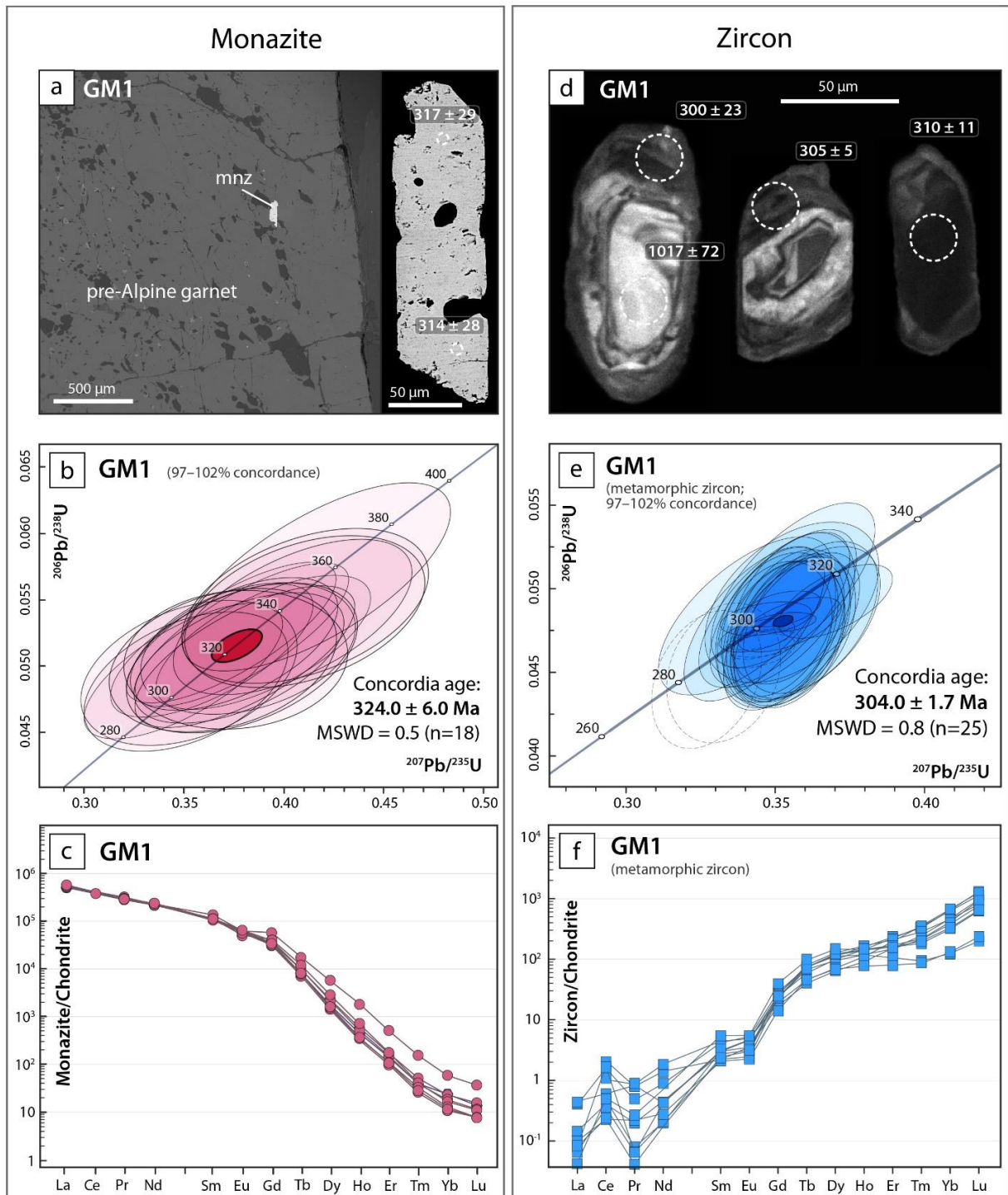


Fig. 9. Legend on next page

Fig. 9. Geochronology of zircon and monazite from garnet-staurolite micaschists constraining the timing of the pre-Alpine cycle. (a) Backscattered electron images of monazite (mnz) included in pre-Alpine garnet rim. On the right-hand side is shown a detail image of an unzoned monazite. Dates are given as $^{206}\text{Pb}/^{238}\text{U}$ dates. (b) Concordia diagram for monazite. (c) Rare earth element (REE) pattern normalized to chondrite (McDonough & Sun, 1995) for monazite. (d) Cathodoluminescence (CL) images of zircon. Zircon displays a detrital core and a metamorphic rim with generally dark CL emission, or is entirely metamorphic. Dates are given as $^{206}\text{Pb}/^{238}\text{U}$ dates. (e) Concordia diagram for metamorphic zircon. (f) REE pattern normalized to chondrite for metamorphic zircon. The heavy-REE pattern displays a positive slope. Modified from paper I (Nosenzo et al., 2022).

We used U-(Th)-Pb dating of monazite and zircon in micaschists from the low-strain domain to obtain timing constraints on two different stages of the pre-Alpine cycle. Pre-Alpine garnet includes anhedral apatite at the core and large subhedral to euhedral monazite at the rim (up to 200 μm ; Fig. 9a). The phosphorous concentration in pre-Alpine garnet, in trace amounts, is low at the core (~ 100 ppm) and increases at the rim (~ 750 ppm). These textural and chemical observations suggest that monazite grew by consumption of apatite during the last stages of pre-Alpine garnet growth, close to peak amphibolite-facies conditions (stage 1 in Fig. 8). Monazite is internally homogeneous in composition and yields a Concordia age of 324 ± 6 Ma (MSWD = 0.5; $n = 18$; Fig. 9a-c).

Zircons display a detrital core and a metamorphic rim (up to ~ 40 μm thick) or are entirely metamorphic (Fig. 9d). The trace element geochemistry of metamorphic zircon is characterized by very low Th/U ratios and a non-flat heavy-rare-earth-element (HREE) pattern (Fig. 9f). The non-flat HREE pattern suggests that metamorphic zircon grew in disequilibrium with garnet, possibly during garnet consumption (e.g. Rubatto, 2002). Metamorphic zircon yields a Concordia age of $\sim 304 \pm 2$ Ma (MSWD = 0.8; $n = 25$; Fig. 9e). Therefore, metamorphic zircon is interpreted to have formed during late pre-Alpine greenschist-facies retrogression (as proposed in different terranes; e.g. Hoiland et al., 2018). Metamorphic zircon growth is likely associated with pre-Alpine garnet dissolution and fluid-rock interactions (stage 2 in Fig. 8, see section 5.6).

In summary, the polycyclic basement of the Muret Unit was involved into the Variscan orogenesis (e.g. Franke et al. 2020). It underwent Barrovian metamorphism up to amphibolite-facies conditions at ~ 324 Ma and subsequent greenschist-facies retrogression at ~ 304 Ma.

5.5 P–T conditions of the Alpine cycle (paper II)

Thermodynamic modelling was used to constrain the Alpine *P–T* evolution of garnet micaschists from low- and high-strain domains. For this purpose, phase diagrams were calculated considering H_2O in excess (H_2O -saturated conditions; e.g. Fig. 10).

Modelling indicates that the studied micaschists experienced the same prograde to peak Alpine evolution; although in different samples Alpine garnet started to grow at slightly different P - T conditions along the prograde path. The Ca-rich garnet inner portion grew during the prograde evolution at 18–20 kbar and 480–500 °C, in the stability field of lawsonite. With increasing T conditions, in fact, the progressive consumption of lawsonite (a Ca-rich silicate) provided a source of Ca for the growing garnet. The grossular isopleths in the field of lawsonite are subhorizontal and, thus, provide a tight constraint on the P . The Ca-poor outer portion equilibrated at peak conditions of 19–23 kbar and 530–560 °C, in absence of lawsonite. At these conditions, the calculated mineral assemblage is consistent with the one observed in the studied samples (g-ctd-gl-mu-ru-q; abbreviations follow Holland & Powell, 1998). In the diagrams, the stability field of this mineral assemblage is bounded at higher P by the appearance of jadeite or carpholite, and at higher T by the appearance of kyanite or the destabilization of chloritoid. The inferred peak T is consistent with the isopleths of chloritoid.

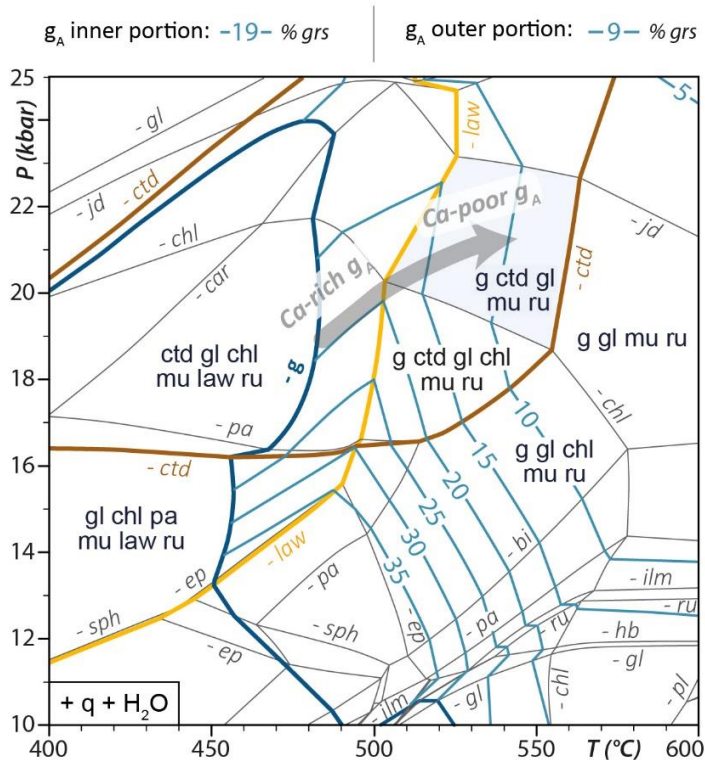


Fig. 10. Isochemical phase diagram used to constrain the Alpine evolution of a polycyclic garnet micaschist (sample GM13). H_2O is considered in excess. Each field (bounded by grey lines) indicates the P - T range where a certain mineral assemblage is stable. Mineral abbreviations follow Holland & Powell (1998). The stability field of the observed peak mineral assemblage (g-ctd-gl-mu-ru-q) is highlighted in pale blue. The boundaries of the stability field of garnet, chloritoid and lawsonite are highlighted with thick blue, brown and yellow lines, respectively. Isopleths of the grossular component in garnet are shown in blue. The grey arrow represents the inferred P - T path of Alpine garnet growth from prograde to peak conditions (stage 3 and 4 in Fig. 8, respectively). Modified from paper II.

In summary we can draw several conclusions from these results: (i) H_2O -saturated conditions are a valid assumption for the Alpine HP overprint, (ii) the observed Alpine garnet zoning is consistent with continuous growth along the prograde to peak path, (iii) micaschists from the Muret

Unit record the same Alpine P - T conditions independently from the intensity of the strain and (iv) the Muret Unit did not reach UHP conditions to the difference of the Chasteiran Unit.

5.6 H_2O budget and rehydration of polycyclic micaschists (paper II)

Thermodynamic modelling was used to quantify the variation in H_2O content in micaschists throughout their polycyclic evolution. Garnet micaschists from the low- and high-strain domains underwent analogous H_2O content evolution.

Along the pre-Alpine prograde path, free H_2O was liberated and the rock progressively dehydrated (stage 1 in Fig. 8). Most H_2O was lost in correspondence of chlorite-consuming reactions. At peak pre-Alpine amphibolite-facies conditions the micaschists contained 1.8–2.3 wt.% mineral-bound H_2O .

T - $M(H_2O)$ diagrams confirm that the observed Alpine HP mineral assemblage and Alpine garnet developed at H_2O -saturated conditions (e.g. Fig. 11). In fact, they show that a weak H_2O undersaturation would have induced the stabilization of anhydrous phases that are not observed in the Alpine mineral assemblage, such as kyanite. In addition, with H_2O -undersaturated conditions the calculated grossular isopleths would be much lower than the measured values in Alpine garnet. However, the H_2O budget inherited from the peak pre-Alpine stage is not enough to guarantee H_2O -saturation during the Alpine overprint. According to T - $M(H_2O)$ diagrams (e.g. Fig. 11), a minimum of 0.7–2.0 wt.% of H_2O must have been added to the rocks after the peak pre-Alpine stage in order to reach H_2O saturation during the Alpine overprint. Comparison of the H_2O content calculated at peak pre-Alpine conditions with the measured loss of ignition (LOI = 2.7–3.1 wt.%; which represents the H_2O content at the end of the Alpine cycle) also suggests a rehydration of ~ 1 wt.%; although this is a qualitative estimate.

Fluid infiltration and rehydration may have occurred mainly at two stages of the polycyclic evolution: (i) during late-Variscan greenschist-facies retrogression (e.g. Floess & Baumgartner, 2013) or (ii) during the Alpine HP overprint (e.g. Engi et al., 2018). The timing of the fluid circulation has important implications for the processes occurring at continental subduction zones (see section 1.7). As discussed in section 5.3, polycyclic garnet textures suggest fluid infiltration associated with chloritization of pre-Alpine garnet during greenschist-facies retrogression (stage 2 in Fig. 8). This LP - LT episode, pre-dating the Alpine HP - LT overprint, may have been recorded also by the staurolite, that was partially replaced by white mica before being pseudomorphed by the Alpine minerals. Micaschists within the low-strain domain are dissected by a network of fractures and brittle-plastic shear zones (metres-long and centimetre-thick) crosscutting the pre-Alpine foliation. Pre-Alpine garnet and staurolite are more intensely dissolved close to these structures. This may suggest that fractures and shear zones acted as fluid pathways. These ductile-brittle structures must be late pre-Alpine in age because (i) they crosscut the pre-Alpine foliation and (ii) Alpine HP minerals in them are randomly-oriented (white mica, chloritoid and pseudomorphed glaucophane), indicating that the Alpine overprint post-dated the deformation

associated with activation of the shear zones. Metamorphic zircon growth at ~ 304 Ma confirms that the main episode of fluid infiltration and pre-Alpine garnet dissolution was associated with the late-Variscan retrogression (see section 5.4). Later, during the Alpine prograde overprint, chlorite was re-transformed into garnet with liberation of H₂O. As a result, H₂O-saturation was attained and the rock progressively dehydrated (stages 3 and 4 in Fig. 8).

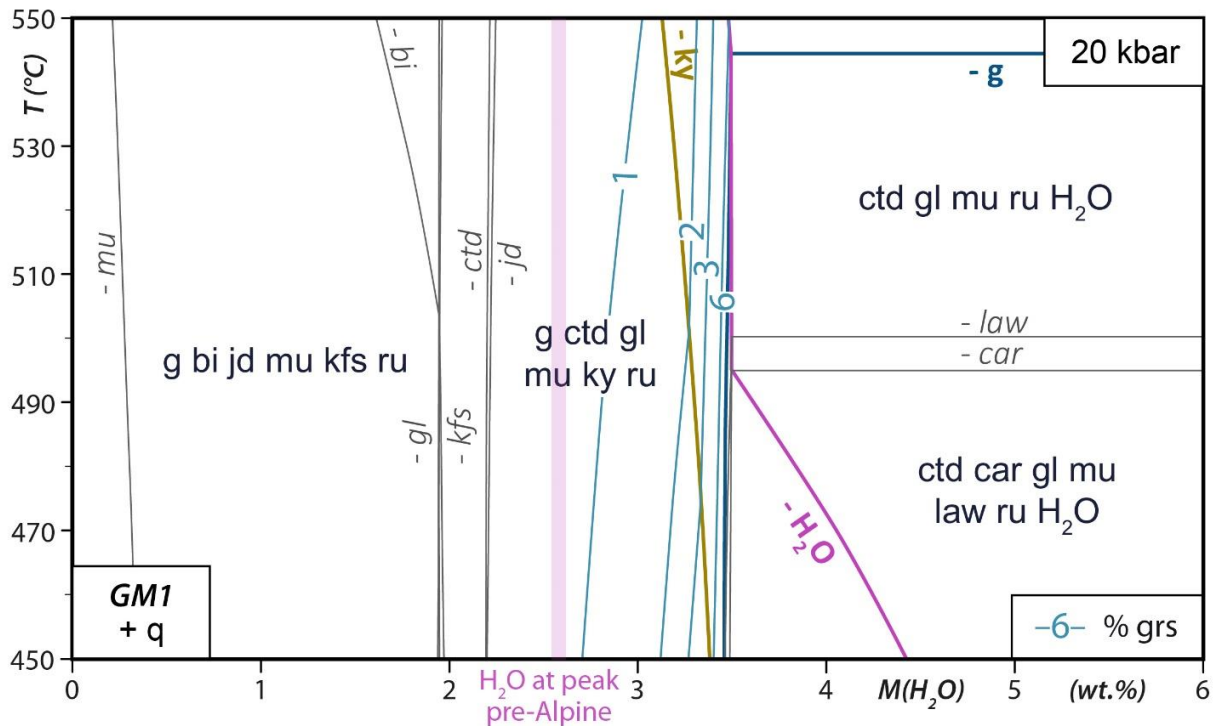


Fig. 11. T - $M(H_2O)$ diagram for the Alpine *HP* overprint of sample GM1. The H₂O saturation line is highlighted in pink and divides the diagram in a H₂O-saturated field to the right and a H₂O-understaturated field on the left. The boundaries of the stability field of garnet and kyanite are highlighted with thick blue and brown lines, respectively. Isopleths of grossular are shown in blue. The pink vertical band represents the calculated H₂O content at peak pre-Alpine conditions for comparison (mineral-bound H₂O + 1 vol.% of free H₂O; porosity from Thompson & Connolly, 1990). A rehydration of ~ 1 wt.% after the peak pre-Alpine stage is needed to reach H₂O-saturation during the Alpine overprint. Modified from paper II.

In other polycyclic terranes, a different scenario invoking fluid infiltration at *HP* conditions has been proposed (e.g. Engi et al., 2018). This has been associated with coupled (i.e. simultaneous) pre-Alpine garnet dissolution and Alpine garnet precipitation (e.g. Giuntoli et al., 2018). According to this model, discontinuous infiltration of fluid pulses results in intermittent Alpine garnet growth and development of irregular zonings. Oscillatory zoning in major and trace element content in Alpine garnet has also been connected with external fluid infiltration in subducting continental crust (e.g. Angiboust et al., 2017). However, such features are not observed

in the studied samples. Instead, Alpine garnet zoning is consistent with continuous growth along the prograde path. We conclude that no major fluid infiltration occurred during the Alpine *HP* overprint.

6. Conclusions and implications for continental subduction

6.1 Reworking of pre-existing continental crust during subduction

6.1.1 Subduction of crustal fragments

We established the tectonic architecture of the northern Dora-Maira Massif and characterized the type and age of its reworked pre-Alpine crust. This allows to make the link with the better-studied southern Dora-Maira Massif and to extend some of the key interpretations and implications.

As a whole, the Dora-Maira Massif comprises the following lithologies in order of abundance: (i) a polycyclic basement of Lower Palaeozoic age, (ii) Upper Carboniferous monocyclic meta-sediments, (iii) Permian monocyclic meta-intrusives and meta-volcaniclastic products and (iv) monocyclic Mesozoic covers. These lithologies are distributed in several tectonic units stacked on top of each other. In both the northern and southern Dora-Maira Massif, the tectonic stack comprises a lower unit of Carboniferous and Permian rocks overthrust by several basement units, in turn overlaid by one or more units with Permian and Mesozoic rocks. As a whole, the metamorphic architecture is consistent in the northern and southern Dora-Maira Massif, with an *UHP* basement unit sandwiched between lower *P* units. Despite the similarities between the tectonic stack in the northern and southern Dora-Maira Massif, the tectonic units in the two sectors are not necessarily equivalents and are likely discontinuous.

The internal architecture of the Dora-Maira Massif implies that the pre-Alpine continental crust was fragmented and subducted in several coherent sheets. Some authors proposed that the tectonic units of the Dora-Maira Massif constituted separated volumes already in the Mesozoic, before the Alpine subduction (Ballèvre et al., 2020; Bonnet et al., 2022). According to this hypothesis, different units occupied a different position along the extended Briançonnais palaeomargin and were bounded by normal faults or, in case they constituted extensional allochthons, by portions of exhumed mantle or oceanic crust. This interpretation is supported by the occurrence of serpentinites and metabasites along the tectonic boundary between some units in both the northern and southern Dora-Maira Massif (e.g. between the Muret Unit and the Serre Unit).

Once involved in the subduction zone, the different crustal fragments were buried at different depths. During exhumation they were juxtaposed with thrusting of the higher *P* units (e.g. the Chasteira Unit) over the lower *P* units (the Pinerolo Unit). Alpine shear zones at their boundaries may have reactivated rift-related normal faults and may have reworked mantle material interposed between extensional allochthons.

6.1.2 Reworking of upper crust

For the first time, we characterized both P – T evolution and age of the pre-Alpine metamorphism in one of the Internal Crystalline Massifs. The polycyclic basement of the northern Dora-Maira Massif underwent Barrovian metamorphism up to the amphibolite facies in connection with the Variscan orogeny. This pre-Alpine episode is analogous for P – T evolution and age to the one recorded in other basement units of the Alps (e.g. Le Bayon et al., 2006; Gaidies et al., 2008; Fréville et al., 2018). However, in some Adria-derived units, such as the Ivrea Zone and some parts of the Sesia - Dent Blanche Nappes (Fig. 2), the Variscan metamorphism (Carboniferous in age) is overprinted by a Permian granulite-facies episode associated with partial melting (Schuster & Stüwe, 2008; Kunz et al., 2018). This indicates that such units resided in the lower crust during the Permian (e.g. Ballèvre et al., 2018). By contrast, the basement of the Dora-Maira Massif did not experience a Permian granulite-facies overprint. In fact, metamorphic zircon growth associated with greenschist-facies retrogression suggests that the basement was already exhumed in the Upper Carboniferous. Therefore, we conclude that the Dora-Maira massif, in both its polycyclic and monocyclic lithologies, consists solely of reworked upper crustal material.

Decoupling of the upper and lower crust may have occurred during the Alpine subduction-exhumation cycle. One possibility is that both the lower and upper crust were subducted but then the latter detached from the downgoing slab and was exhumed, whereas the former remained at depth (e.g. Guillot et al., 2009). Alternatively, decoupling may have occurred before the Alpine history, during Mesozoic extension. Asymmetric Mesozoic rifting may be responsible for the occurrence of upper crustal material in the Briançonnais margin (Dora-Maira Massif) and of exhumed lower crustal material the Adriatic margin (as represented in Fig. 1; e.g. Ballèvre et al., 2020). This interpretation, plausible for the Dora-Maira Massif, supports a model where the part of the continental crust that is most deeply subducted and exhumed is the thinned distal margin.

6.2 The role of H₂O during subduction of polycyclic crust

We retraced the variation in H₂O budget of polycyclic micaschists throughout two orogenic cycles. Because micaschists are the predominant lithology in the Muret Unit, we can consider these results as generally valid for the polycyclic unit as a whole.

Over the course of the first orogenic cycle, Variscan in age, the polycyclic crust of the northern Dora-Maira Massif was firstly dehydrated during prograde Barrovian metamorphism (~ 324 Ma) and subsequently rehydrated during retrogression and cooling (~ 304 Ma). Rehydration was likely the result of percolation of aqueous fluids along Late Variscan fractures and consequent replacement of anhydrous minerals by hydrous ones (e.g. chlorite replacing garnet).

During subduction and prograde metamorphism in connection with the second orogenic cycle (Alpine), fluids were liberated by the breakdown of hydrous minerals (e.g. chlorite). Such internally-derived fluid was enough to allow the development of the *HP* mineral assemblage. The

Alpine garnet zoning in the studied meta-pelites, is the result of continuous growth along the prograde evolution and does not exhibit chemical modifications caused by interactions with externally-derived fluid pulses.

With respect to the two models of fluid-rock interactions at continental subduction zones described in section 1.7, we conclude that the polycyclic crust of the Dora-Maira Massif behaved according to the first model. The polycyclic crust dehydrated during subduction with minor release internally-derived fluid. The essentially closed system behaviour of the polycyclic crust respect to external fluid infiltration during subduction has been inferred by other authors in other units of the Alps (e.g. Schorn, 2018). Although, in these terranes the crust is thought to not have rehydrated after the peak pre-Alpine stage.

These findings may be valid only for the upper continental crust such as that of the Dora-Maira Massif, which had the chance rehydrate before subduction. The relatively high H₂O budget of the rehydrated upper crust allowed pervasive metamorphic re-equilibration during subduction. By contrast, a dry lower crust such as the one found in some Adria-derived units of the Alps may have equilibrated only upon encountering externally-derived fluids during subduction, according to the second fluid-rock interaction model (e.g. Engi et al., 2018).

In the studied rocks, during the late-Alpine exhumation, partial replacement of garnet by chlorite along late-stage fractures was likely triggered by local fluid infiltration from an external source, as documented in other subducted and exhumed continental terranes (e.g. Masago et al., 2010; Konrad-Schmolke et al., 2011; Massonne, 2012).

References

- Ampferer, O. (1906). Über das Bewegungsbild von Faltengebirgen. *Jahrbuch der Kaiserlich-königlichen Geologischen Reichsanstalt*, 56, 539–622.
- Amstutz, A. (1951). Sur l'évolution des structures Alpines. *Archives des Sciences (Genève)*, 4, 323–329.
- Andersen, T. (2005). Detrital zircons as tracers of sedimentary provenance: Limiting conditions from statistics and numerical simulation. *Chemical Geology*, 216, 249–270.
- Angiboust, S., Yamato, P., Hertgen, S., Hyppolito, T., Bebout, G. R., & Morales, L. (2017). Fluid pathways and high-P metasomatism in a subducted continental slice (Mt. Emilius klippe, W. Alps). *Journal of Metamorphic Geology*, 35, 471–492.
- Argand, E. (1916). Sur l'arc des Alpes Occidentales. *Eclogae Geologicae Helvetiae*, 14, 145–191.
- Austrheim, H. (1987). Eclogitization of lower crustal granulites by fluid migration through shear zones. *Earth and Planetary Science Letters*, 81, 221–232.
- Austrheim, H. (2013). Fluid and deformation induced metamorphic processes around Moho beneath continent collision zones: Examples from the exposed root zone of the Caledonian mountain belt, W-Norway. *Tectonophysics*, 609, 620–635.
- Austrheim, H., Erambert, M., & Engvik, A. K. (1997). Processing of crust in the root of the Caledonian continental collision zone: the role of eclogitization. *Tectonophysics*, 273, 129–153.
- Ballèvre, M., Camonin, A., Manzotti, P., & Poujol, M. (2020). A step towards unraveling the paleogeographic attribution of pre-Mesozoic basement complexes in the Western Alps based on U–Pb geochronology of Permian magmatism. *Swiss Journal of Geosciences*, 133, 12.
- Ballèvre, M., Manzotti, P., & Dal Piaz, G. V. (2018). Pre-Alpine (Variscan) inheritance: A key for the location of the future Valais Basin (Western Alps). *Tectonics*, 37, 786–817.
- Barrow, G. (1893). On an intrusion of muscovite-biotite gneiss in the south-eastern highlands of Scotland, and its accompanying meta-morphism. *Quarterly Journal of the Geological Society*, 49, 330–358.
- Baxter, E. F., & Caddick, M. J. (2013). Garnet growth as a proxy for progressive subduction zone dehydration. *Geology*, 41, 643–646.
- Becquerel, A. (1896). Émission de radiations Nouvelles par l'uranium métallique. *Comptes Rendus de l'Académie de Sciences de Paris*, 122, 1086.
- Bjørnerud, M. G., Austrheim, H., & Lund, M. G. (2002). Processes leading to eclogitization (densification) of subducted and tectonically buried crust. *Journal of Geophysical Research*, 107, 2252.
- Bhowany, K., Hand, M., Clark, C., Kelsey, D. E., Reddy, S. M., Pearce, M. A., Tucker, N. M. & Morrissey, L. J. (2018). Phase equilibria modelling constraints on P–T conditions during fluid catalysed conversion of granulite to eclogite in the Bergen Arcs, Norway. *Journal of Metamorphic Geology*, 36, 315–342.

- Bonnet, G., Chopin, C., Locatelli, M., Kyander-Clark, A., & Hacker, B. R. (2022). Protracted subduction of the European hyperextended margin revealed by rutile U-Pb geochronology across the Dora-Maira massif (W. Alps). *Tectonics*, 41, e2021TC007170.
- Borghi, A., Cadoppi, P., Porro, A., & Sacchi, R. (1985). Metamorphism in the northern part of the Dora-Maira Massif (Cottian Alps). *Bollettino del Museo Regionale di Scienze Naturali*, Torino, 3, 369–380.
- Bouffette, J., Lardeaux, J. M., & Caron, J. M. (1993). Le passage des granulites aux éclogites dans les métapelites de l'unité de la Punta Muret (Massif Dora-Maira, Alpes occidentales). *Comptes Rendus de l'Académie des Sciences de Paris Serie II*, 317, 1617–1624.
- Burov, E., Francois, T., Yamato, P., & Wolf, S. (2012). Mechanisms of continental subduction and exhumation of HP and UHP rocks. *Gondwana Research*, 25, 464–493.
- Bussy, F., & Cadoppi, P. (1996). U-Pb dating of granitoids from the Dora-Maira massif (western Italian Alps). *Schweizerische Mineralogische Und Petrographische Mitteilungen*, 76, 217–233.
- Butler, J. P., Beaumont, C., & Jamieson, R. A. (2014). The Alps 2: Controls on crustal subduction and (ultra)high-pressure rock exhumation in Alpine-type orogens. *Journal of Geophysical research: Solid Earth*, 119, 5987–6022.
- Caddick, M. J., Konopásek, J., & Thompson, A. B. (2010). Preservation of garnet growth zoning and the duration of prograde metamorphism. *Journal of Petrology*, 51, 2327–2347.
- Cadoppi, P. (1990). *Geologia del Basamento Cristallino nel Settore Settentrionale del Massiccio Dora-Maira (Alpi Occidentali)*. PhD's thesis. 208 pp.
- Carlson, W.D. (2002). Scales of disequilibrium and rates of equilibration during metamorphism. *American Mineralogist*, 87, 185–204.
- Carlson, W. D. (2010). Dependence of reaction kinetics on H₂O activity as inferred from rates of intergranular diffusion of aluminium. *Journal of Metamorphic Geology*, 28, 735–752.
- Carlson, W.D., Pattison, D. R. M., & Caddick, M. J. (2015). Beyond the equilibrium paradigm: How consideration of kinetics enhances metamorphic interpretation. *American Mineralogist*, 100, 1659–1667.
- Cherniak, D. J., & Watson, E. B. (2001). Pb diffusion in zircon. *Chemical Geology*, 172, 5–24.
- Chopin, C. (1984). Coesite and pure pyrope in high-grade blueschists of the Western Alps: a first record and some consequences. *Contributions to Mineralogy and Petrology*, 84, 107–118.
- Chopin, C., Henry, C., & Michard, A. (1991). Geology and petrology of the coesite-bearing terrain, Dora-Maira massif, Western Alps. *European Journal of Mineralogy*, 3, 263–291.
- Cocco, F., Oggiano, G., Funedda, A., Loi, A., & Casini, L. (2018). Stratigraphic, magmatic and structural features of Ordovician tectonics in Sardinia (Italy): A review. *Journal of Iberian Geology*, 44, 619–639.
- Compagnoni, R., & Rolfo, F. (2003). UHPM Units in the Western Alps. Ultrahigh-Pressure Units in the Western Alps. In D. A. Carswell & R. Compagnoni (Eds.), *Ultrahigh-pressure metamorphism*, European Mineralogical Union Notes in Mineralogy (Vol. 5, pp. 13–49). Eötvös University Press.

- Compagnoni, R., Rolfo, F., Groppo, C., Hirajima, T., & Turello, R. (2012). Geological map of the ultra-high pressure Brossasco-Isasca unit (Western Alps, Italy). *Journal of Maps*, 8, 465–472.
- Connolly, J. A. D. (2010). The mechanics of metamorphic fluid expulsion. *Elements*, 6, 165–172.
- Curie, P., & Sklodowska-Curie, M. (1898). Sur une substance nouvelle radio-active contenue dans le pechblende. *Comptes Rendus de l'Academie de Sciences de Paris*, 127, 175–178.
- Cutts, K. A., Kinny, P. D., Strachan, R. A., Hand, M., Kelsey, D. E., Emery, M., Friend, C. R. L., & Leslie, G. (2010). Three metamorphic events recorded in a single garnet: Integrated phase modelling, in situ LA-ICPMS and SIMS geochronology from the Moine Supergroup, NW Scotland. *Journal of Metamorphic Geology*, 28, 249–267.
- De Capitani, C., & Petrakakis, K. (2010). The computation of equilibrium assemblage diagrams with Theriak/Domino software. *American Mineralogist*, 95, 1006–1016.
- Doin, M.-P., & Henry, P. (2001). Subduction initiation and continental crust recycling: the roles of rheology and eclogitization. *Tectonophysics*, 342, 163–191.
- Engi, M., Giuntoli, F., Lanari, P., Brun, M., Kunz, B., & Bouvier, A.-S. (2018). Pervasive Eclogitization Due to Brittle Deformation and Rehydration of Subducted Basement: Effects on Continental Recycling? *Geochemistry, Geophysics, Geosystems*, 19, 865–881.
- Engi, M., Lanari, P., & Kohn, M. J. (2017). Significant Ages—An Introduction to Petrochronology. *Reviews in Mineralogy and Geochemistry*, 83, 1–12.
- Evans, T. P. (2004). A method for calculating effective bulk composition modification due to crystal fractionation in garnet-bearing schist: implications for isopleth thermobarometry. *Journal of Metamorphic Geology*, 22, 547–557.
- Fedo, C. M., Sircombe, K. N., & Rainbird, R. H. (2003). Detrital zircon analysis of the sedimentary record. *Reviews in Mineralogy and Geochemistry*, 53, 277–303.
- Ferry, J. M., & Gerdes, M. L. (1998). Chemically activated fluid flow during metamorphism. *Annual Reviews of Earth and Planetary Sciences*, 26, 255–287.
- Ferry, J. M., & Spear, F. S. (1978). Experimental calibration of the partitioning of Fe and Mg between biotite and garnet. *Contribution to Mineralogy and Petrology*, 66, 113–117.
- Fielding, C. R. (2021). Late Palaeozoic cyclothems – A review of their stratigraphy and sedimentology. *Earth-Science Reviews*, 217, 103612.
- Floess, D., Baumgartner, L., (2013). Formation of garnet clusters during polyphase metamorphism. *Terra Nova*, 25, 144–150.
- Franke, W., Ballèvre, M., Cocks, L. R. M., Torsvik, T. H., & Żelaźniewicz, A. (2020). Variscan orogeny. In *Encyclopedia of Geology* (2nd ed.). Elsevier.
- Fréville, K., Trap, P., Faure, M., Melleton, J., Li, X.-H., Lin, W., Blein, O., Bruguier, O., & Poujol, M. (2018). Structural, metamorphic and geochronological insights on the Variscan evolution of the Alpine basement in the Belledonne Massif (France). *Tectonophysics*, 726, 14–42.
- Frisch, W., Meschede, M., & Blakey, R. (2011). *Plate tectonics*. Springer, Berlin. 212 pp.
- Fryer, B. J., Jackson, S. E., & Longgerich, H. P. (1993). The application of laser ablation microprobe-inductively coupled plasma-mass spectrometry (LA-ICP-MS) to in situ (U)-Pb geochronology. *Chemical Geology*, 109, 1–8.

- Gaidies, F., Abart, R., De Capitani, C., Schuster, R., Connolly, J. A. D., & Reusser, E. (2006). Characterization of polymetamorphism in the Austroalpine basement east of the Tauern Window using garnet isopleth thermobarometry. *Journal of Metamorphic Geology*, 24, 451–475.
- Gaidies, F., Krenn, E., De Capitani, C., & Abart, R. (2008). Coupling forward modelling of garnet growth with monazite geochronology: An application to the Rappold Complex (Austroalpine crystalline basement). *Journal of Metamorphic Geology*, 26, 775–793.
- Gaidies, F., Morneau, Y. E., Petts, D. C., Jackson, S. E., Zagorevski, A., & Ryan, J. J. (2020). Major and trace element mapping of garnet: Unravelling the conditions, timing and rates of metamorphism of the Snowcap assemblage, west-central Yukon. *Journal of Metamorphic Geology*, 39, 133–164.
- Ganguly, J. (2010). Cation diffusion kinetics in aluminosilicate garnets and geological applications. *Reviews in Mineralogy and Geochemistry*, 72, 559–601.
- Gardés, E., Wunder, B., Marquardt, K., & Heinrich, W. (2012). The effect of water on intergranular mass transport: new insights from diffusion-controlled reaction rims in the MgO–SiO₂ system. *Contributions to Mineralogy and Petrology*, 164, 1–16.
- Gasco, I., Gattiglio, M., & Borghi, A. (2011). Lithostratigraphic setting and P-T metamorphic evolution for the Dora-Maira Massif along the Piedmont Zone boundary (middle Susa Valley, NW Alps). *International Journal of Earth Sciences*, 100, 1065–1085.
- Gerya, T. (2015). Tectonic overpressure and underpressure in lithospheric tectonics and metamorphism. *Journal of Metamorphic Geology*, 33, 785–800.
- Giuntoli, F., Lanari, P., Engi, M., 2018. Deeply subducted continental fragments-Part 1: fracturing, dissolution-precipitation, and diffusion processes recorded by garnet textures of the central Sesia Zone (western Italian Alps). *Solid Earth*, 9, 167–167.
- Goldschmidt, V. M. (1912). *Die Gesetze der Gesteinsmetamorphose: Norsk Videnskapselskaps Skrifter I. Matematisk-Naturvidenskapelig Klasse*, 22. 16 pp.
- Green, H. W. (1994). Solving the paradox of deep earthquakes. *Scientific American*, 271, 50–57.
- Groppo, C., Beltrando, M., & Compagnoni, R. (2009). The P–T path of the ultra-high pressure Lago Di Cignana and adjoining high-pressure meta-ophiolitic units: insights into the evolution of the subducting Tethyan slab. *Journal of Metamorphic Geology*, 27, 207–231.
- Groppo, C., Ferrando, S., Gilio, M., Botta, S., Nosenzo, F., Balestro, G., Festa, A., & Rolfo, F. (2019). What's in the sandwich? New P–T constraints for the (U)HP nappe stack of southern Dora-Maira Massif (Western Alps). *European Journal of Mineralogy*, 31, 665–683.
- Guillot, S., Hattori, K., Agard, P., Schwartz, S., & Vidal, O., (2009). Exhumation processes in oceanic and continental subduction contexts: a review. In Lallemand, S., Funicello, F. *Subduction Zone Geodynamics*, 175–205.
- Guiraud, M., Powell, R., & Rebay, G. (2001). H₂O in metamorphism and unexpected behaviour in the preservation of metamorphic assemblages. *Journal of Metamorphic Geology*, 19, 445–454.

- Handy, M. R., Schmid, S. M., Bousquet, R., Kissling, E., & Bernoulli, D. (2010). Reconciling plate-tectonic reconstructions of Alpine Tethys with the geological–geophysical record of spreading and subduction in the Alps. *Earth-Science Reviews*, 102, 121–158.
- Handy, M. R., Schmid, S. M., Paffrath, M., Friederich, W., & the AlpArray Working Group (2021). Orogenic lithosphere and slabs in the greater Alpine area – interpretations based on teleseismic P-wave tomography. *Solid Earth*, 12, 2633–2021.
- Hensen, B. J., & Essene, E. J. (1971). Stability of pyrope-quartz in the system MgO-Al₂O₃-SiO₂. *Contributions to Mineralogy and Petrology*, 30, 72–83.
- Hoiland, C. W., Miller, E. L., & Pease, V. (2018). Greenschist facies metamorphic zircon overgrowths as a constraint on exhumation of the Brooks Range metamorphic core. *Alaska Tectonics*, 37, 3429–3455.
- Holland, T. J. B., & Powell, R. (1998). An internally consistent thermodynamic data set for phases of petrological interest. *Journal of Metamorphic Geology*, 16, 309–343.
- Hollister, L. S. (1966). Garnet zoning: An interpretation based on the Rayleigh fractionation model. *Science*, 154, 1647–1651.
- Holmes, A. (1911). The association of lead with uranium in rock-minerals and its application to the measurement of geologic time. *Proceedings of the Royal Society of London*, 85, 248–256.
- Hoskin, P. W. O., & Schaltegger, U. (2003). The composition of zircon and igneous and metamorphic petrogenesis. *Reviews in Mineralogy and Geochemistry*, 53, 27–62.
- Hirata, T., & Nesbitt, R. W. (1995). Isotope geochronology of zircon: evaluation of laser probe-inductively coupled plasma mass spectrometry technique. *Geochimica et Cosmochimica Acta*, 59, 2491–2500.
- Ingalls, M., Rowley, D. B., Currie, B., & Colman, A. S. (2016). Large-scale subduction of continental crust implied by India–Asia mass-balance calculation. *Nature Geoscience*, 9, 848–853.
- Inui, M., & Toriumi, M. (2004). A theoretical study on the formation of growth zoning in garnet consuming chlorite. *Journal of Petrology*, 45, 1369–1392.
- Jolivet, L., Raimbourg, H., Labrousse, L., Avigad, D., Leroy, Y., Austrheim, H., & Andersen, T. B. (2005). Softening triggered by eclogitization, the first step toward exhumation during continental subduction. *Earth and Planetary Science Letters*, 237, 532–547.
- Kearey, P., Klepeis, K. A., & Vine, F. J. (2009). *Global tectonics*. Wiley-Blackwell, Oxford. 496 pp.
- Konrad-Schmolke, M., O'Brien, P. J., & Zack, T. (2011). Fluid migration above a subducted slab—constraints on amount, pathways and major element mobility from partially overprinted eclogite-facies rocks (Sesia Zone, Western Alps). *Journal of Petrology*, 52, 457–486.
- Kunz, B. E., Manzotti, P., von Niederhäusern, B., Engi, M., Darling, J. R., Giuntoli, F., Lanari, P. (2018). Permian high-temperature metamorphism in the Western Alps (NW Italy). *International Journal of Earth Sciences*, 107, 203–229.

- Lanari, P., & Duesterhoeft, E. (2019). Modeling Metamorphic Rocks Using Equilibrium Thermodynamics and Internally Consistent Databases: Past Achievements, Problems and Perspectives. *Journal of Petrology*, 60, 19–56.
- Lang, H. M., & Gilotti, J. A. (2015). Modeling the exhumation path of partially melted ultrahigh-pressure metapelites, North-East Greenland Caledonides. *Lithos*, 131–146.
- Le Bayon, B., Pitra, P., Ballèvre, M., & Bohn, M. (2006). Reconstructing P–T paths during continental collision using multi-stage garnet (Gran Paradiso nappe, Western Alps). *Journal of Metamorphic Geology*, 24, 477–496
- Li, Z. H., Gerya, T. V., & Burg, J.-P., (2010). Influence of tectonic overpressure on P-T paths of HP-UHP rocks in continental collision zones: thermomechanical modelling. *Journal of Metamorphic Geology*, 28, 227–247
- Liou, J. G., Tsujimori, T., Zhnag, R. Y., Katayama, I., & Maruyama, S. (2004). Global UHP metamorphism and continental subduction/collision: the Himalayan model. *International Geology Reviews*, 46, 1–27.
- Liu, F. L., Gerdes, A., & Xue, H. M. (2009). Differential subduction and exhumation of crustal slices in the Sulu HP-UHP metamorphic terrane: insights from mineral inclusions, trace elements, U-Pb and Lu-Hf isotope analyses of zircon in orthogneiss. *Journal of Metamorphic Geology*, 27, 805–825.
- Ludwig, K. R. (1998). On the treatment of concordant uranium-lead ages. *Geochimica et Cosmochimica Acta*, 62, 665–676.
- Luisier, C., Baumgartner, L., Schmalholz, S. M., Siron, G., & Vennemann, T. (2019). Metamorphic pressure variation in a coherent Alpine nappe challenges lithostatic pressure paradigm. *Nature Communications*, 10, 4734.
- Lund, M. G., & Austrheim, H. (2003). High-pressure metamorphism and deep-crustal seismicity: evidence from contemporaneous formation of pseudotachylytes and eclogite facies coronas. *Tectonophysics*, 372, 59–83.
- Malusà, M. G., Carter, A., Limoncelli, M., Villa, I. M., & Garnzanti, E. (2013). Bias in detrital zircon geochronology and thermochronometry. *Chemical Geology*, 359, 90–107.
- Malvoisin, B., Austrheim, H., Hetényi, G., Reynes, J., Hermann, J., Baumgarthner, L. P., & Podladchikov, Y. Y. (2020). Sustainable densification of the deep crust. *Geology*, 47, 7.
- Manzotti, P., & Ballèvre, M. (2013). Multistage garnet in high-pressure metasediments: Alpine overgrowths on Variscan detrital grains. *Geology*, 41, 1151–1154.
- Manzotti, P., Ballèvre, M., & Poujol, M. (2016). Detrital zircon geochronology in the Dora-Maira and Zone Houillère: A record of sediment travel paths in the Carboniferous. *Terra Nova*, 28, 279–288.
- Manzotti, P., Schiavi, F., Nosenzo, F., Pitra, P., Ballèvre, M. (2022). A journey towards the forbidden zone: a new cold UHP unit in the Dora-Maira Massif (Western Alps). *Contributions to Mineralogy and Petrology*, 177, 59.

- Masago, H., Omori, S., & Maruyama, S. (2010). Significance of retrograde hydration in collisional metamorphism: A case study of water infiltration in the Kokchetav ultrahigh-pressure metamorphic rocks, northern Kazakhstan. *Gondwana Research*, 18, 205–212.
- Massonne, H.-J. (2012). Formation of amphibole and clinozoisite–epidote in eclogite owing to fluid infiltration during exhumation in a subduction channel. *Journal of Petrology*, 53, 1969–1998.
- Mattey, D., Jackson, D. H., Harris, N. B. H., & Kelley, S. (1994). Isotopic constraints on fluid infiltration from an eclogite facies shear zone, Holsenøy, Norway. *Journal of Metamorphic Geology*, 12, 311–325.
- Mattirolo, E., Novarese, V., Franchi, S., Stella, A. (1913). Carta Geologica d'Italia alla scala 1:100.000, Foglio 67 Pinerolo. Geological Survey of Italy.
- Mattirolo, E., Novarese, V., Franchi, S., Stella, A. (1951). Carta Geologica d'Italia alla scala 1:100.000, Foglio 67 Pinerolo. Geological Survey of Italy.
- McDonough, W. F., & Sun, S. S. (1995). The composition of the Earth. *Chemical Geology*, 120, 223–253.
- McKenzie, D. P. (1969). Speculations on the consequences and causes of plate motions. *Geophysical Journal International*, 18, 1–32.
- Michard, A., Schmid, S. M., Lahfid, A., Ballèvre, M., Manzotti, P., Chopin, C., Iaccarino, S., & Dana, D. (2022). The Maira-Sampeyre and Val Grana allochthons (south Western Alps): review and new data on the tectonometamorphic evolution of the Briançonnais distal Margin. *Swiss Journal of Geosciences*, 115, 19.
- Milke, R., Neusser, G., Kolzer, K., & Wunder, B. (2013). Very little water is necessary to make a dry solid silicate system wet. *Geology*, 41, 247–250.
- Müller, R. O. (1972). *Spectrochemical Analysis by X-Ray Fluorescence*. Plenum Press. 325 pp.
- Nosenzo, F., Manzotti, P., Pujol, M., Ballèvre, M., & Langlade, J. (2022). A window into an older orogenic cycle: P–T conditions and timing of the pre-Alpine history of the Dora-Maira Massif (Western Alps). *Journal of Metamorphic Geology*, 40(4), 789–821.
- Otamendi, J. E., de la Rosa, J. D., Patiño Douce, A. E., & Castro, A. (2002). Rayleigh fractionation of heavy rare earths and yttrium during metamorphic garnet growth. *Geology*, 30(2), 159–162.
- Parrish, R. R. (1990). U-Pb dating of monazite and its application to geological problems. *Canadian Journal of Earth Sciences*, 27.
- Passchier, C. W., & Trouw, R. A. J. (2005). *Microtectonics*. Springer, 366 pp.
- Pattison, D. R. M., De Capitani, C., & Gaides, F. (2011). Petrological consequences of variations in metamorphic reaction affinity. *Journal of Metamorphic Geology*, 29, 953–977.
- Pettke, T., Diamond, L. W., & Kramers, J. D. (2000). Mesothermal gold lodes in the north-western Alps: a review of genetic constraints from radiogenic isotopes. *European Journal of Mineralogy*, 12, 213–230.
- Powell, R., & Holland, T. J. B. (1994): Optimal geothermometry and geobarometry. *American Mineralogist*, 79, 120–133.

- Powell, R., Holland, T., & Worley, B. (1998). Calculating phase diagrams involving solid solutions via non-linear equations, with examples using THERMOCALC: *Journal of Metamorphic Geology*, 16, 577–588.
- Prior, D. J. (1993). Sub-critical fracture and associated retrogression of garnet during mylonitic deformation. *Contributions to Mineralogy and Petrology*, 113, 545–556.
- Proyer, A. (2003). The preservation of high-pressure rocks during exhumation: metagranites and metapelites. *Lithos*, 70, 183–194.
- Putnis, A., Moore, J., Prent, A. M., Beinlich, A., & Austerheim, H. (2021). Preservation of granulite in a partially eclogitized terrane: Metastable phenomena or local pressure variations?. *Lithos*, 400–401.
- Rao, S. E., Ray, L., Khan, T., & Ravi, G. (2022). Thermal conductivity, density and porosity of sedimentary and metamorphic rocks from the Lower and Higher Himalaya, Western Himalaya, India. *Geophysical Journal International*, 231, 459–473.
- Reed, S. J. B. (2005). *Electron microprobe analysis and scanning electron microscopy in geology*. Cambridge University Press, Cambridge. 190 pp.
- Rolfo, F., Compagnoni, R., Wu, W., & Xu, S. (2004). A coherent lithostratigraphic unit in the coesite–eclogite complex of Dabie Shan, China: geologic and petrologic evidence. *Lithos*, 73, 71–94.
- Rubatto, D. (2002). Zircon trace element geochemistry: partitioning with garnet and the link between U–Pb ages and metamorphism. *Chemical Geology*, 184, 123–138.
- Rubatto, D. (2017). Zircon: The Metamorphic Mineral. *Reviews in Mineralogy and Geochemistry*, 83, 261–295.
- Rubatto, D., & Hermann, J. (2001). Exhumation as fast as subduction? *Geology*, 29, 3–6.
- Rubie, D. C. (1986). The catalysis of mineral reactions by water and restrictions on the presence of aqueous fluid during metamorphism. *Mineralogical Magazine*, 50, 399–415.
- Sandrone, R., Cadoppi, P., Sacchi, R., & Vialon, P. (1993). The Dora-Maira massif. In *Pre-Mesozoic geology in the Alps* (pp. 317–325). Springer.
- Sandrone, R., Trogolo Got, D., Respino, D., & Zucchetti, S. (1987). Osservazioni geogiacimentologiche sulla miniera di talco di Fontane (Val Germanasca, Ali Cozie). *Memorie di Scienze Geologiche (Padova)*, 39, 175–186.
- Schenker, F. L., Schmalholz, S. M., Moulas, E., Pleuger, J., Baumgartner, L. P., Podladchikov, Y., Vrijmoed, J., Buchs, N., & Müntener, O. (2015). Current challenges for explaining (ultra)high-pressure tectonism in the Pennine domain of the Central and Western Alps. *Journal of Metamorphic Geology*, 33, 869–886.
- Schmalholz, S. M., & Podladchikov, Y. Y. (2014). Metamorphism under stress: the problem of relating minerals to depth. *Geology*, 42, 733–734
- Schmalholz, S. M., & Schenker, F. (2016). Exhumation of the Dora Maira ultrahigh-pressure unit by buoyant uprising within a low-viscosity mantle oblique-slip shear zone. *Terra Nova*, 28, 348–355.

- Schmid, S. M., Fügenschuh, B., Kissling, E., & Schuster, R. (2004). Tectonic map and overall architecture of the Alpine orogeny. *Eclogae Geologicae Helvetiae*, 97, 93–117.
- Schmidt, M. W., & Poli, S. (1998). Experimentally based water budgets for dehydrating slabs and consequences for arc magma generation. *Earth and Planetary Science Letters*, 163, 361–379.
- Schneider, F. M., Tuan, X., Schurr, B., Mechie, J., Sippl, C., Haberland, C., Minaev, V., Oimahmadov, I., Gadoev, M., Radjabov, N., Abdybachaev, U., Orunbaev, S., & Negmatullaev, S., (2013). Seismic imaging of subducting continental lower crust beneath the Pamir. *Earth and Planetary Science Letters*, 375, 101–112.
- Schorn, S. (2018). Dehydration of metapelites during high-P metamorphism: the coupling between fluid sources and fluid sinks. *Journal of Metamorphic Geology*, 36, 369–391.
- Schorn, S. (2022). Self-induced incipient ‘eclogitization’ of metagranitoids at closed-system conditions. *Journal of Metamorphic geology*, 40, 1271–1290.
- Schuster, R., & Stüwe, K. (2008). Permian metamorphic event in the Alps. *Geology*, 36, 603–606.
- Smith, D. C. (1984). Coesite in clinopyroxene in the Caledonides and its implications for geodynamics. *Nature*, 310, 641–644.
- Tenczer, V., Powell, R., & Stüwe, K. (2006). Evolution of H₂O content in a polymetamorphic terrane: the Plattengneiss Shear Zone (Koralpe, Austria). *Journal of Metamorphic Geology*, 24, 281–295.
- Thompson, J. B., Jr. (1955). The thermodynamic basis for the mineral facies concept: *American Journal of Science*, 253, 65–103.
- Thompson, A. B., & Connolly, J. A. D. (1990). Metamorphic fluids and anomalous porosities in the lower crust. *Tectonophysics*, 182, 47–55.
- Tullborg, E.L., & Larson, E. A. (2006). Porosity in crystalline rocks – A matter of scale *Engineering Geology*, 84, 75–83.
- Vermeesch, P. (2004). How many grains are needed for a provenance study? *Earth and Planetary Science Letters*, 224, 441–451.
- Vialon, P. (1966). Etude géologique du massif cristalline Dora-Maira, Alpes Cottiennes Internes, Italie. Grenoble: Travaux du Laboratoire de Géologie de la Faculté des Sciences de Grenoble, Mémoires.
- Villa, I. M., & Hanchar, J. M. (2017). Age discordance and mineralogy. *American mineralogist*, 102, 2422–2439.
- Vine, F. J., & Matthews, D. H. (1963). Magnetic anomalies over oceanic ridges. *Nature*, 199, 947–949.
- Vho, A., Rubatto, D., Lanari, P., Giuntoli, F., Regis, D. & Hermann, J. (2020). Crustal reworking and hydration: insights from element zoning and oxygen isotopes of garnet in high-pressure rocks (Sesia Zone, Western Alps). *Contribution to Mineralogy and Petrology*, 175, 109.
- Wain, A. L., Waters, D. J., & Austrheim, H. (2001). Metastability of granulites and processes of eclogitisation in the UHP region of western Norway. *Journal of Metamorphic Geology*, 19, 609–625.

- Walther, J. V., & Oreville, P. M. (1982). Volatile production and transport in regional metamorphism. *Contribution to Mineralogy and Petrology*, 79, 252–257.
- Watson, E. B., Cherniak, D. J., Hanchar, J. M., Harrison, T. M., Wark, D. A. (1997). The incorporation of Pb into zircon. *Chemical Geology*, 141, 19–31.
- Wegener, A. (1912). Die Entstehung der Kontinente. *Geologische Rundschau*, 3, 276–292.
- Wetherill, G. W. (1954). Variations in the isotopic abundances of neon and argon extracted from radioactive minerals. *Physical Review*, 96, 679–683.
- Yamato, P., Burov, E., Agard, P., Le Pourhiet, L., & Jolivet, L. (2008). HP-UHP exhumation during slow continental subduction: Self-consistent thermodynamically and thermomechanically coupled model with application to the Western Alps. *Earth and Planetary Science Letters*, 271, 63–74.
- Young, D. J., & Kylander-Clark, R. C. (2015). Does continental crust transform during eclogite facies metamorphism? *Journal of Metamorphic Geology*, 33, 331–357.
- Zertani, S., Labrousse, L., John, T., Andersen, T. B., & Tilmann, F. (2019). The Interplay of Eclogitization and Deformation During Deep Burial of the Lower Continental Crust—A Case Study From the Bergen Arcs (Western Norway). *Tectonics*, 38, 898–915.
- Zhao, L., Paul, A., Guillot, S., Solarino, S., Malusà, M. G., Zheng, T., Aubert, C., Salimbeni, S., Dumont, T., Schwartz, S., Zhu, R., & Wang, Q. (2015). First seismic evidence for continental subduction beneath the Western Alps. *Geology*, 43, 815–818.

Acknowledgements

First and foremost, I thank my supervisor Paola Manzotti who has been an influential presence throughout my PhD studies. Among the things that I have learnt from her I want to mention the great dedication to research work and the meticulous attention to details in scientific writing. Secondly, I thank Michel Ballèvre for always inspiring me to be a curious and engaged scientist. Our field work together has been very enriching. A special mention goes to Victoria Pease who has always offered quality help on both scientific and administrative matters. Sincere gratitude goes to Malin Kylander for guiding me throughout the PhD adventure. I thank Alasdair Skelton for the internal evaluation of this thesis and Joakim Mansfeld for the help with the translation of the abstract in Swedish. I am grateful to all the co-authors of the papers comprised in this thesis. I thank the K & A Wallenbergs Stiftelse 2019, C F Liljevalch J:ors stipendiefond 2021 and Rhodnis Minne 2022 for funding a large part of the field work and conferences.

My experience at the Department of Geological Sciences (IGV) and with the people that give life to it has been very positive. In particular I thank the community of PhD students, MSc students and post-docs and the Geologklubben, with which I have spent nice moments of work and entertainment. Many are the people who have been part of this; some are still at IGV and some already left. In particular, I thank Robert Dunst, Simone Seminara and Kevin Hatton for sharing most of my PhD adventures and William Westin, Mikaela Krona and Vidar Jakobsson for sharing part of the field work, lab work and conference trips. Thanks also to the other professors and the technical and administrative staff at IGV. I am very grateful to the Erasmus Program for giving me the opportunity to come in contact with IGV and Stockholm University (SU) already during my MSc studies.

Finally, I thank all the people that have been close to me during this four-year period and, thus, have directly or indirectly contributed to its success. PhD students and post-docs from the Department of Organic Chemistry and the Department of Meteorology at SU have adopted me as a friend. Bridging between the academic world and the outside world, I have found my “angel” in Alba Ambròs, whose experience in mentoring has been of great help. Outside the academic world I thank all my friends that are scattered around the globe, in particular my old friend Giuseppe. Fundamental during the last part of my PhD studies has been the concrete support of Minu, who I cannot thank enough. Lastly, I am grateful to my parents, my sister and the rest of my family for providing the most solid base for any further development.